THE ROLE OF FLT3 IN HEPATOCELLULAR CARCINOGENESIS

A THESIS SUBMITTED TO

THE DEPARTMENT OF MOLECULAR BIOLOGY AND GENETICS

AND THE INSTITUTE OF ENGINEERING AND SCIENCE OF

BILKENT UNIVERSITY

IN PARTIAL FULFILLMENT OF THE REQUIREMENTS FOR

THE DEGREE OF MASTER OF SCIENCE

BY

N. SUMRU BAYIN

JULY 2010

I certify that I have read this thesis and that in my opinion it is fully adequate, in scope and in quality, as a thesis for the degree of Master of Science.

_____

Assist. Prof. Dr. K. Can Akçalı

I certify that I have read this thesis and that in my opinion it is fully adequate, in scope and in quality, as a thesis for the degree of Master of Science.

_____

Assoc. Prof. Dr. İhsan Gürsel

I certify that I have read this thesis and that in my opinion it is fully adequate, in scope and in quality, as a thesis for the degree of Master of Science.

_____

Assoc. Prof. Dr. Cengiz Yakıcıer

Approved for the Institute of Engineering and Science

_____

Director of Institute of Engineering and Science

Prof. Dr. Levent Onural

ABSTRACT

THE ROLE OF FLT3 IN HEPATOCELLULAR CARCINOGENESIS

N. Sumru BAYIN

M.S. in Molecular Biology and Genetics

Supervisor: Assist. Prof. Dr. K. Can Akçalı

July 2010, 82 Pages

Hepatocellular carcinoma (HCC) is one of the most prevalent cancer types and it has a high mortality rate. Its high incidence is a consequence of lack of biomarkers that could track the progression of the disease. Identification of a marker, which involves in different stages of cancer progression, through fibrosis to HCC, would be a good candidate for diagnosis, prediction of prognosis and targeted therapies. Therefore we decided to identify a novel marker for HCCs, to overcome these consequences. Previously our group has shown that oval cell marker FLT3, a known hematopoetic stem cell marker and which is known to be constitutively active in many of the leukemias, has a role in liver regeneration. Also our immunohistochemical analysis of cirrhotic liver tissues have shown that FLT3 is expressed in liver injury. Therefore, we decided to analyze the role of FLT3 in hepatocellular carcinogenesis. Expression analysis of FLT3 on mRNA and protein level and the expression analysis of adult stem cell, cancer stem cell, and epithelial and mesenchymal lineage markers on mRNA level in 14 HCC cell lines (HepG2, Hep3B, Hep40, Huh7, PLC/PRF/5, Mahlavu, Focus, Sk-Hep-1, Snu182, Snu387, Snu398, Snu423, Snu449, Snu475) was performed. Four of these cell lines (Snu182, Snu398, Huh7 and Hep40) were chosen due to their different expression levels of FLT3 and the functional role of FLT3 in HCCs was assessed by blocking its activity by a small molecule inhibitor K-252a *Nocardiopsis* sp.. Functional studies had shown that upon inhibitor treatment, subcellular localization of the protein was changed and its invasion ability *in vitro* was impaired. Also nude mice xenografts had shown that upon inhibitor treatment tumor forming ability of FLT3 expressing cells were highly diminished. Therefore we suggest that FLT3 has a role in hepatocellular carcinogenesis and it might be another link between liver regeneration and hepatocellular carcinogenesis.

Keywords: Hepatocellular carcinoma, liver Regeneration, FLT3.

ÖZET

FLT3'ÜN KARACİĞER KANSERİNDEKİ ROLÜ

N. Sumru BAYIN

Moleküler Biyoloji ve Genetik Yüksek Lisans

Tez Yöneticisi: Yar. Doç. Dr. K. Can Akçalı

Temmuz 2010, 82 Sayfa

Karaciğer kanseri, dünyada en yaygın görülen ve ölüm oranı çok yüksek olan bir hastalıktır. Bu durumunun başlıca sebebi de, kanseri tanısında ve tedavisinde etkili olacak genlerin çok iyi tanımlanmamış olmasından kaynaklanır. Karaciğer kanserinin fibrozdan baslayan farklı aşamalarında rolü bulunan genelerin tanımlanması, kanseri tanısında, seyirinin tespitinde ve tedavisinde önemli gelişmeler sağlayacaktır. Bu nedenle yeni bir belirleyici gen bulmayı amaçlamaktayız. Grubumuzun daha önceki çalışmasında, oval hücre belirleyicisi olan FLT3 geninin karaciğer yenilenmesi sırasında bir rolü olduğu gösterilmiştir. FLT3'ün kan kök hücrelerinde bulunduğu ve kan kanserlerinde ifade ve aktivitelerinde artış olduğu bilinmektedir. İmunohistokimyasal analizlerimiz ile FLT3'ün sirotik karaciğerler de gözlemlediğimiz için, bu genenin karaciğer yaralanmalarının yanısıra karaciğer kanserinde de rolü olduğunu düşünmekteyiz. Bu amaçla, 14 karaciğer kanseri hücre hattında (HepG2, Hep3B, Hep40, Huh7, PLC/PRF/5, Mahlavu, Focus, Sk-Hep-1, Snu182, Snu387, Snu398, Snu423, Snu449, Snu475), FLT3'ün mRNA ve protein düzeyinde, diğer erişkin kök hücre ve kanser kök hücresi belirleyicilerinin de mRNA düzeyinde ifadelerini araştırdık. Daha sonra FLT3 ifadesinin çeşitliliğine göre 4 hücre hattı (Snu182, Snu398, Huh7 ve Hep40) belirleyip, bunlarda FLT3 inhibitörü kullanarak, genin fonksiyonunu inceledik. Inhibitör, protenin hücre içindeki yerini değiştirmekle birlikte, bu hücrelerin *in vitro* ortamda yayılmalarında da değişikliğe sebep olmuştur. Bunun yanı sıra çıplak farelerdeki zenograft deneyleri, FLT3 ifadesi gösteren hücrelerin inhibitöre maruz kaldıklarında tümör oluşturma etkilerinde büyük ölçüde azalma görülmüştür. Bu sonuçlar bize FLT3'in karaciğer kanserlerinde önemli rol oynadığını göstermekte ve FLT3'ün karaciğer yenilenmesi ve kanseri arasında bir bağ kurabileceğini düşündürmektedir.

Anahtar Kelimeler: Karaciğer kanseri, karaciğer yenilenmesi, FLT3.

ACKNOWLEDGEMENTS

I would like to express my gratitude to my supervisor Assoc. Prof. Dr. Can Akçalı for his personal and academic guidance and for his trust in me. I hope I didn't let him down, in any part of this study. It was an honor for me to work with him.

I would like to thank the present and former members of Akçalı Group, Zeynep Tokcaer Keskin, Fatma Ayaloğlu Bütün, Verda Bitirim, Sinan Gültekin and Hande Koçak for their friendship, support and patience in answering my endless questions. I couldn't accomplish this without their help.

I would like to thank to Assist. Prof Dr. Cengiz Yakıcer for his ideas and support during this thesis research. Also I would like to thank to Tolga Acun for his help and providing the cell lines.

I would like to thank to Assoc. Prof. Dr. İhsan Gürsel for his supervision and members of İG group for their help.

I would like to thank to MBG faculty, for providing me the necessary background that I will need in my future endeavors.

I would like to thank to Chigdem, Aslı, Ceren, Gizem, Emre, my classmates and all the MBG family members, who made this journey joyful and easy, for their support, friendship and help.

I would like to thank The Scientific and Technological Research Council of Turkey (TÜBİTAK) for their financial support throughout my studies with BIDEB 2210 Scholarship.

I would like to thank to Aslı, Begüm, Elvan, Gizem and Nil for being more than friends. Finally, I would like to thank to my dear parents for always believing in me and for supporting my decisions no matter what.

TABLE OF CONTENTS

ABSTRACT ..... **II**

ÖZET ..... **III**

ACKNOWLEDGEMENTS ..... **IV**

TABLE OF CONTENTS ..... **V**

LIST OF TABLES ..... **VIII**

LIST OF FIGURES ..... **IXX**

ABBREVIATIONS ..... **XI**

1. INTRODUCTION **1**

1.1 LIVER 2

1.1.1 Liver Development *2*

1.1.2 Liver Anatomy and Histology *4*

1.1.3. Epithelial-Mesenchymal Transitions *7*

1.1.4 Liver Regeneration *9*

1.1.5 Liver Fibrosis *10*

1.1.6 Cirrhosis *11*

1.1.7 Hepatocellular Carcinoma *11*

1.2 FMS-LIKE TYROSIN KINASE (FLT3) 14

1.2.1 Structure of FLT3 ..... *14*

1.2.2 FLT3 Signal Transduction *15*

1.2.3 Physiological Functions of FLT3 ..... *17*

1.2.4 Pathophysiological Functions of FLT3 ..... *18*

2. AIM OF THE STUDY **20**

3. MATERIALS AND METHODS **21**

3.1 CELL CULTURE 21

3.1.1 K-252a Treatment of HCC cell lines *21*

3.2 NUDE-MICE TUMOR XENOGRAFTS 21
3.3 STANDARD BUFFERS AND SOLUTIONS 22
3.4 TOTAL RNA ISOLATION 22
3.5 CDNA SYNTHESIS 23
3.6 REVERSE TRANSCRIPTASE-POLYMERASE CHAIN REACTION (RT-PCR) 23
3.6.1 Multiplex PCR for Sip1/Zeb2 and GAPDH 26
3.6.2 Agarose Gel Electrophoresis 27
3.7 PROTEIN ISOLATION 27
3.7.1 Total Protein Isolation 27
3.7.2 Protein Quantification with Bradford Assay 28
3.8 WESTERN BLOTTING 28
3.8.1 SDS-Polyacrylamide Gel Electrophoresis (SDS-PAGE) 28
3.8.2 Transfer of Proteins to the PVDF Membrane 29
3.8.3 Immunological Detection of Immobilized Proteins 30
3.9 IMMUNOSTAINING PROCEDURES 31
3.9.1 Immunohistochemistry Staining for Paraffin Embedded Tissue Sections 31
3.9.2 Immunoflourescense Staining for Frozen Tissue Sections 32
3.9.3 Immunoflourescense Staining 32
3.10 WOUND HEALING ASSAY 33
3.11 TUNEL ASSAY 33
3.12 SENESCENCE ASSOCIATED B-GAL ASSAY (SABG) 34
3.13 STATISTICAL ANALYSIS 35
4. RESULTS 36
4.1 CHARACTERIZATION OF HCC CELL LINES 36
4.1.1 Expression Pattern of FLT3 in HCC Cell Lines 36
4.1.2 Expression Analysis of Adult Stem Cell, Cancer Stem Cell and Hematopoietic Lineage Markers in 14 HCC Cell Lines 38
4.1.3 Expression Analysis of Epithelial and Mesenchymal Lineage Markers in 14 HCC Cell Lines with RT-PCR 39
4.2 EXPRESSION OF FLT3 IN CIRRHOTIC AND NORMAL HUMAN LIVER 39

4.3 FUNCTIONAL ANALYSIS OF FLT3 IN HCCS BY INHIBITING THE PHOSPHORYLATION OF THE PROTEIN WITH K-252A 41
4.3.1. Effect of K-252a on the cellular morphology in HCCs 42
4.3.2 Effect of K-252a on the Subcellular Localization of FLT3 in HCCs 42
4.3.3 Wound Healing Assay 44
4.3.4 Change in the Epithelial and Mesenchymal Lineage Markers After Inhibitor Treatment 48
4.3.5 In vitro Programmed Cell Death Analysis and Senescence Associated β-Gal Assay 49
4.4 *IN VIVO* TUMORIGENESIS 52
5. DISCUSSION 57
5.1 DISCUSSION 57
5.2 FUTURE PERSPECTIVES 66
6. REFERENCES 67
7. APPENDIX 76

LIST OF TABLES

TABLE 3. 1 PRIMERS USED FOR EXPRESSION ANALYSIS IN RT-PCR....24
TABLE 3. 2 REACTION MIXTURE FOR RT-PCR....25
TABLE 3. 3 REACTION MIXTURE OF SIP1-GAPDH MULTIPLEX RT-PCR....26
TABLE 3. 4 BSA STANDARD CURVE FOR BRADFORD ASSAY....29
TABLE 3. 5 ANTIBODIES USED FOR WESTERN BLOTTING ANALYSIS. 30
TABLE 3. 6 SECONDARY ANTIBODIES USED IN WESTERN BLOTTING....30
TABLE 3. 7 PREPARATION OF SABG SOLUTION 35
TABLE 3. 8 PREPARATION OF NA-P BUFFER....35
TABLE 5. 1 FINDINGS OF *IN VITRO* AND *IN VIVO* EXPERIMENTS....65

LIST OF FIGURES

FIGURE 1. 1 FLOWCHART SHOWING THE EMBRYONIC DEVELOPMENT OF THE LIVER 4
FIGURE 1. 2 STRUCTURE OF A LIVER LOBULE 5
FIGURE 1. 3 A CLOSER VIEW OF THE LIVER LOBULE AND CELL TYPES FOUND IN THE LIVER 6
FIGURE 1. 4 MOLECULAR MARKERS INVOLVED IN EPITHELIAL MESENCHYMAL TRANSITION 8
FIGURE 1. 5 MECHANISMS FOR HEPATOCELLULAR CARCINOGENESIS 12
FIGURE 1. 6 FLT3 STRUCTURE 15
FIGURE 1. 7 DOWNSTREAM EFFECTORS OF FLT3 19
FIGURE 4. 1 EXPRESSION PROFILING OF FLT3 WITH RT-PCR 37
FIGURE 4. 2 WESTERN BLOTTING ANALYSIS WITH FLT3 ANTIBODY 37
FIGURE 4. 3 EXPRESSION PROFILING OF 14 HCC CELL LINES FOR ADULT STEM CELL, CANCER STEM CELL AND HEMATOPOIETIC CELL LINEAGE MARKERS. 38
FIGURE 4. 4 RT-PCR ANALYSIS FOR EPITHELIAL AND MESENCHYMAL LINEAGE MARKERS. 39
FIGURE 4. 5 FLT3 IMMUNOHISTOCHEMISTRY OF A NORMAL LIVER 40
FIGURE 4. 6 FLT3 IMMUNOHISTOCHEMISTRY OF A CIRRHOTIC LIVER. 41
FIGURE 4. 7 INVERTED MICROSCOPY PHOTOS OF SNU182 AND SNU398 AFTER 200NM INHIBITOR TREATMENT FOR TWO HOURS. 42
FIGURE 4. 8 FLT3 IMMUNOFLOUROSCENCE 43
FIGURE 4. 9 PHOTOGRAPHS OF WOUND HEALING ASSAY FOR SNU182 44
FIGURE 4. 10 STATISTICAL ANALYSIS OF WOUND HEALING CAPACITY OF SNU182 45
FIGURE 4. 11 PHOTOGRAPHS OF WOUND HEALING ASSAY FOR SNU398 46
FIGURE 4. 12 STATISTICAL ANALYSIS OF WOUND HEALING CAPACITY OF SNU398 46
FIGURE 4. 13 PHOTOGRAPHS OF WOUND HEALING ASSAY FOR HUH7 47
FIGURE 4. 14 STATISTICAL ANALYSIS OF WOUND HEALING CAPACITY OF HUH7 48
FIGURE 4. 15 RT-PCR ANALYSIS OF EPITHELIAL AND MESENCHYMAL LINEAGE MARKERS AFTER 200NM K-252A TREATMENT FOR TWO HOURS. 49
FIGURE 4. 16 THE RATIO OF APOPTOTIC INDICES OF INHIBITOR TREATED CELLS AND DMSO TREATED CELLS. 50
FIGURE 4. 17 SABG STAINING OF SNU182, SNU398, HUH7 AND HEP40 51
FIGURE 4. 18 XENOGRAFT TUMORS OF SNU398. 53
FIGURE 4. 19 XENOGRAFT TUMORS OF HEP40. 54
FIGURE 4. 20 XENOGRAFT TUMORS OF HUH7. 55

FIGURE 4. 21 AVERAGE TUMOR VOLUMES OF XENOGRAFTS INJECTED WITH SNU398, HEP40 AND HUH7 CELLS IN THE PRESENCE OR ABSENCE OF INHIBITOR. 56
FIGURE 5. 1 FLT3'S INVOLVEMENT DURING DIFFERENT STAGES LEADING TO HCC 64

ABBREVIATIONS

2-AAF: N-2-acetylaminofluorene

AML: Acute Myloid Leukemia

BMP: Bone Morphogenic Proteins

bp: base pair

BSA: Bovine Serum Albumin

cDNA: complementary DNA

CSC: Cancer Stem Cell

DC: Dendritic Cell

ddH_2O: double distilled water

DMEM: Dulbecco's Modified Eagle Medium

DNA: deoxyribonucleic acid

DNAse: Deoxribonuclease

EMT: Eptihelial-Mesenchymal Transition

ESC: Embryonic Stem Cell

FLT3: Fms-like Tyrosine Kinase 3

FLT3L: FLT3 Ligand

HBV: Hepatitis B Virus

HCC: Hepatocellular Carcinoma

HCV: Hepatitis C Virus

HGF: Hepatocyte Growth Factor

ITD: Internal Tandem Duplication

kDa: Kilo Dalton

MET: Mesenchymal-Epithelial Transition

MSC: Mesenchymal Stem Cell

µL: Microliter

mL: Milliliter

nM: nanoMolar

NS: non-significant

OD: Optical Density

PH: Partial Hepatectomy

pmol: picomol

RNA: ribonucleic acid

rpm: revolution per minute

RPMI: Roswell Park Memorial Institute medium

RTK: Receptor Tyrosine Kinase

RT: Room Temperature

RT-PCR: Reverse Transcriptase Polymerase Chain Reaction

TKD: Tyrosine Kinase Domains

TUNEL: Terminal d-UTP Nick End Labeling

X-Gal: 5-bromo-4-chloro-3-indolyl-β-D-galactoside

1. Introduction

Its functional importance and regenerative capacity make liver one of the most interesting organ in the body. Liver was considered as the principle organ and the first organ to be formed in the fetus by the medieval scientists (http://www.stanford.edu/class/history13/earlysciencelab/body/liverpages/livergallbladderspleen.html). Its regenerative capacity has been recognized even earlier times, illustrated by the ancient Greek legend of Prometheus. In the myth of Prometheus, after stealing the fire from Zeus for the mortals, he had been punished by being tied in a rock in Caucasus Mountain and having a part of its liver eaten by a great eagle. According to the myth his liver was regenerating everyday so that the eagle can eat it (Michalopoulos and DeFrances, 1997).

Liver is very important for the survival of the organism and perturbation of its functions causes very severe consequences. Only cure for its end-stage diseases is the liver transplantation. Among these conditions, Hepatocellular Carcinoma (HCC) has one of the highest incidence rates all over the world. HCC is the second most lethal cancer after pancreatic cancer according to the statistics of 2005. Even more alarming is the fact that incidence and death rates from HCC are increasing since 1980s and there is an estimated 18.910 liver cancer deaths in America for the year 2010 (American Cancer Society, http://www.cancer.org/downloads/STT/Cancer_Facts_and_Figures_2010.pdf).

Lack of biomarkers for early prognosis, as well as targeted therapies and resistance to chemotherapeutic agents are some of the important reasons of its high incidence and lethality.

This drawback has urged us to identify a candidate marker for HCC. Fms-like Tyrosine Kinase (FLT3) is a hematopoietic stem cell marker, which is important for the development of the hematopoietic cells and also its aberrant

functioning leads to different types of leukemia. Although it seems there is no close relation between FLT3 and the liver, as we trace the steps of liver development, liver regeneration and HCC throughout this thesis, the relation will reveal itself, and the rationale behind this thesis can be easily understood.

Introduction section starts with a brief explanation of the liver development. Then the anatomy and the functioning units of the liver and the different types of cells found in the liver will be explained. Later on, processes of liver regeneration, fibrosis and HCC will be discussed and the role of FLT3 and epithelial-mesenchymal transition will be mentioned in each context. Finally, the structural and functional properties of FLT3 will be analyzed.

1.1 Liver

Liver is the largest organ in the body and its functions and structure make it a vital organ throughout the development and the adult life. Liver has several important functions such as glycogen storage, drug detoxification, cholesterol and urea metabolism, the production and secretion of hormones (such as Insulin-like Growth Factor, Angiotensinogen and Thrombopoietin) as well as plasma proteins such as Albumin and Apolipoproteins. In addition to its endocrine function, liver also has exocrine secretion in the form of bile (Si-Tayeb et al, 2010).

1.1.1 Liver Development

Throughout the development and during the adult life, stem cells play very important roles in the maintenance of the tissues both anatomically and physiologically. Stem cells are specialized cells that are capable of self-renewing themselves and differentiating into cells of different lineages. During development, embryonic stem cells (ESC) are found in the inner cell mass of the blastula of a day 4 embryo. These cells are pluripotent stem cells that are able to give rise to a whole organism, except the extra-embryonic tissues in mammalian

development (Evans and Kaufman, 1981; Martin, 1981). As the development proceeds, the first liver bud is observed in embryonic day 8.5, which expresses some hepatic markers such as Albumin and Hnf4a, a transcription factor, which is expressed in early hepatic cells (Bort et al, 2006).

As the embryonic day 8.5 is reached in mammalian development, the signals from the septum transversum mesenchyme direct the tissue specific foregut endodermal progenitor cells to differentiate into liver bud and form the hepatoblast. The collective effect of fibroblast growth factors from the cardiac mesoderm and bone morphogenic proteins (BMP) from the septum transversum exhibits their function by the activation of transcription factors such as Hex, GATA and FoxA. Hex has an evolutionary role in the development of the liver bud and it is activated by SMAD1 and SMAD4, which make it a direct target of BMP signaling (Zhang et al, 2007). GATA and FoxA function during the remodeling of the chromatin structure in the promoter region of Albumin. Coordinately, the development of the hepatic vasculature is very important for the expansion of the liver bud (Zhao and Duncan, 2005). The Kupffer cells derived from the yolk sac emerge in the sinusoidal capillaries (Enzan et al, 1983) and hepatic stellate cells are also derived from septum transversum mesenchymal cells (Wandzioch et al, 2004).

There are a wide variety of signals involved in the liver development. The major signal involved in liver growth is Wnt signaling, which promotes the formation of bipotential liver progenitor cells. These cells eventually differentiate in two different cell lineages: (1) hepatocytes and (2) cholangiocytes on embryonic day 16, via Notch signaling and hepatocyte growth factor (HGF) signaling respectively. Besides Notch and HGF signaling, TGF-β also provides necessary signals for the growth of the fetal liver (Mishra et al, 2009) (Figure 1.1).

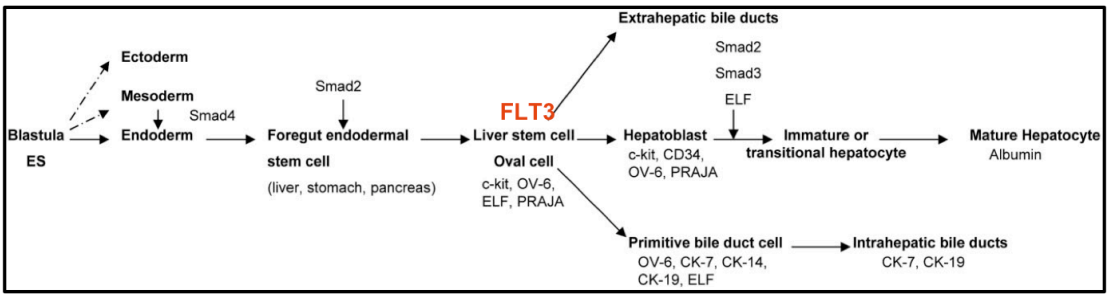

Figure 1. 1 Flowchart showing the embryonic development of the liver (adapted from Mishra et al, 2009)

During development, fetal liver is also the primary site for hematopoiesis between embryonic day 11.5 and 16.5, which suggest a close relationship between the hematopoietic cells and the hepatic parenchyma. The interchange of signals between the hematopoietic cells within the fetal liver and the hepatocytes are crucial for the development of both cell types. Oncostatin M secreted from hematopoietic cells induces hepatocyte differentiation via increased HNF4α expression and co-culturing of fetal hepatocytes with hematopoietic cells showed increased growth and proliferation of hematopoietic cells (Kinoshita et al, 1999).

FLT3 is hematopoietic lineage marker and FLT3 signaling stimulates myeloid and lymphoid progenitor cell proliferation. The close relation of hematopoietic stem cells during liver development and hematopoiesis also implies that FLT3 signaling can also function in the interplay of these two processes.

1.1.2 Liver Anatomy and Histology

Liver consists of lobules, which contains hepatocytes, vascular tissues and bile ducts. Hepatocytes are the most abundant cell type in liver. Portal vein and hepatic artery supply the blood through the sinusoidal capillaries (Figure 1.2).

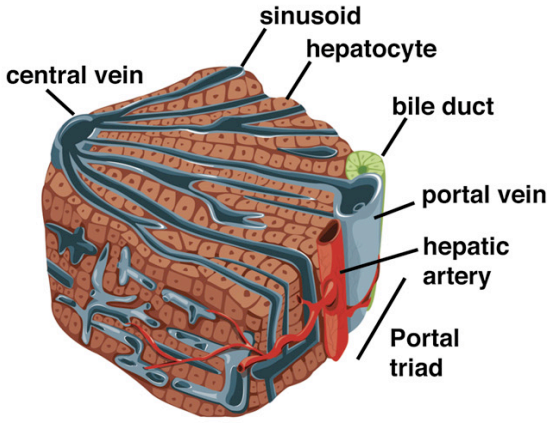

Figure 1. 2 Structure of a liver lobule (Si-Tayeb et al, 2010)

Although the parenchyma of the liver is hepatocytes, there are many other cell types in the liver to fulfill its function. Other than hepatocytes, liver consists of cholangiocytes (biliary epithelial cells), endothelial cells, sinusoidal endothelial cells, Kupffer cells (resident liver macrophages), pit cells (natural killer cells), and hepatic stellate cells (Figure 1.3).

Approximately 78% of the paranchyme volume of the liver is hepatocytes (Blouin et al, 1977). Hepatocytes are epithelial cells, and they perform most of the functions of the liver ranging from protein secretion, bile secretion, detoxification, cholesterol, urea and glucose/glycogen metabolisms.

Cholangiocytes are located in the duct epithelium of the liver and their main function is to form the bile ducts for the transport of bile. The physical properties such as the rate of the bile flow and the pH of the bile are controlled by cholangiocytes. Also they have the ability to secrete water and bicarbonate to contribute to liver homeostasis.

Endothelial cells form the vasculature of the liver, and supply the blood. Sinusoidal endothelial cells help the detoxification of the liver by transferring molecules, proteins and macromolecule wastes between serum and hepatocytes.

Pit cells and Kupffer cells involve in the immune functions of the liver. Pit cells perform cytotoxic activity and the kupffer cells secrete cytokines and proteases and they are the antigen presenting cells (Si-Tayeb et al, 2010).

Finally hepatic stellate cells maintain the extracellular matrix, and most importantly they contribute to the regeneration process through hepatic fibrosis, where the activation of stellate cells leads fibrosis. Also they are sites for retinoic acid storage (Friedman, 2008).

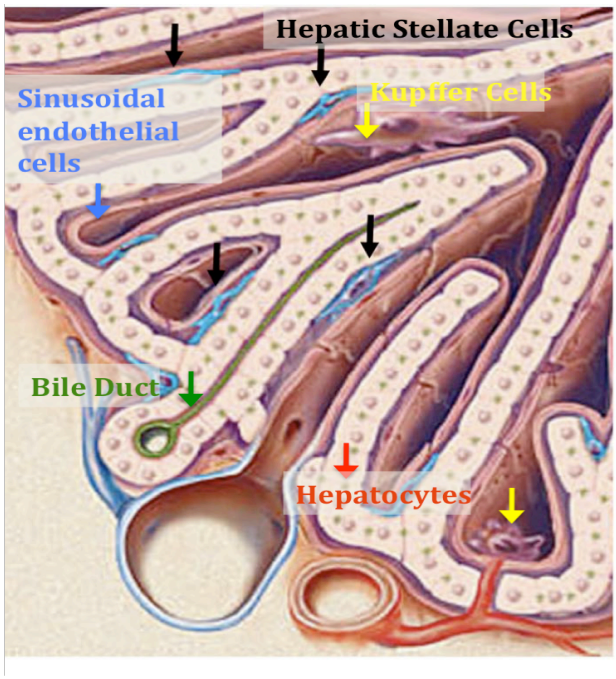

Figure 1. 3 A closer view of the liver lobule and cell types found in the liver (adapted from Freidman, 2008)

On the other hand, in adult liver, there are hepatic progenitor cells, which lie in the Canals of Herring, the biliary trees of the liver, in direct contract with the hepatocytes and bile duct cells. These cells are equivalent to the rodent "oval cells" (Sell and Leffer, 2008; Mishra et al, 2009).

Oval cells express a wide range of markers, which include hepatocyte lineage markers, cholangiocyte lineage markers and even some hematopoietic lineage markers such as c-kit (Mishra et al, 2009) and FLT3 (Aydin et al, 2007) (Figure 1.1).

These bipotential progenitor cells, which express markers of both fetal hepatocytes and biliary cells, are able to differentiate into both lineages. They have the ability to differentiate into hepatocytes and biliary cell but they can only perform this action when the hepatocyte proliferation is stalled, as in the case of a toxic chemical exposure to induce liver regeneration (Fausto and Campbell, 2003). Therefore these cells have critical importance in the success of regeneration process.

Upon the injury, survival of the organism partly depends on a biological process called Epithelial-Mesenchymal Transition (EMT).

1.1.3. Epithelial-Mesenchymal Transitions

Epithelial-Mesenchymal Transition (EMT) is a normal physiological process that takes place during embryonic development. The reverse process of the EMT is called Mesenchymal-Epithelial Transition (MET). EMT/MET during embryogenesis is responsible for the formation mesodermal and endodermal mesenchyme, secondary epithelia and more. These two processes define changes in the cell's shape and adhesive properties not their cell fate. The process involves a change in the genetic programming of the polarized epithelial cells into mobile mesenchymal cells. Epithelial cells are polarized cells with apical and basolateral sides, and they are tightly attached to each other with tight and adherens junctions. Mesenchymal cells on the other hand form when the epithelial cells loose their apico-basolateral polarity and junctions. Many markers are established to differentiate epithelial and mesenchymal cells. Loss of E-cadherin (E-cad) is a global marker for EMT (Figure 1.4) (Kalluri and Weinberg, 2009).

EMT/MET is observed during embryogenesis (Type 1 EMT), wound healing/tissue regeneration/organ fibrosis (Type 2 EMT) and neoplasia (Type 3 EMT) (Kalluri and Weinberg, 2009; Choi and Diehl, 2009). In our context, we will concentrate on its involvement in tissue regeneration and neoplasia.

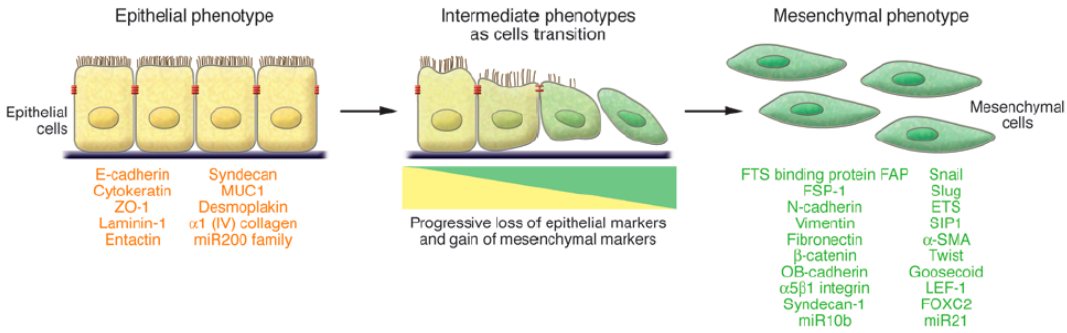

Figure 1. 4 Molecular Markers involved in Epithelial Mesenchymal Transition (Kalluri and Weinberg, 2009)

During injury and fibrosis, as the inflammation response is activated and sustained, EMT produces fibroblastic cells that cause progressive fibrosis. Which cells undergo EMT to produce fibroblasts is controversial but there are evidences for hepatocytes that undergo EMT via TGF-β1 stimulation (Zeisberg et al, 2007). Not only hepatocytes but also cholangiocytes are also undergoing EMT upon fibrosis and this process is regulated by Hedgehog signaling (Omenetti et al, 2008).

The outcome of the EMT/MET process during fibrosis is critical for the repair process. If the incidence of MET is more, this means that epithelial cells are formed, which are hepatocytes and cholangiocytes in this case, the repair successful and regeneration is achieved but if EMT predominates the process, excessive fibrosis occurs (Choi and Diehl, 2009).

1.1.4 Liver Regeneration

Besides its important functions mentioned above, liver is a unique organ with its regenerative capacity. Liver regeneration can be induced by partial hepatectomy (PH) or liver injury by CCl_4 treatment (Hermandez-Munoz et al, 1990), which induces hepatocyte death and fibrosis.

PH is the surgical procedure first defined by Higgins and Anderson in 1931, where 2/3 of the livers of the animals are removed. Upon this procedure in rodents, it is observed that animals can restore their original liver volume in a week and then stop regenerating. Also liver performs this action by not producing a new lobe, but by increasing the volume of the existing lobe/lobes (Taub, 2004). This technique is still being widely used in liver regeneration experiments. How liver maintains its volume and how this regeneration is enabled are still questions that need to be answered, although the evidences are accumulating. There are different types of mechanisms involved in the liver regeneration upon PH. These can be summarized as:

- Replication of existing hepatocytes: Hepatocytes are normally non-dividing cells, but when subjected to PH, remaining 95% of the hepatocytes re-enter into the cell cycle, to restore the liver volume (Michalopoulos and DeFrances, 1997).

- Progenitor cell-dependent regeneration: After some types of injuries, such as intraperitoneal injection of D-galactosamine (GaIN) or treatment with N-2-acetylaminofluorene (2-AAF), hepatocytes cannot proliferate. In such cases, the progenitor cells of the liver proliferate and differentiate into mature hepatocytes (Dabeva and Shafritz, 1993). These progenitor cells are namely oval cells (in rodents) or hepatic progenitor cells (in human) (Taub, 2004).

- Homing of bone marrow derived mesenchymal stem cells (MSC) to the site of injury: When MSCs isolated from bone marrow of the rats are

labeled and reinjected to rats with liver injury, they are found to be located in the site of injury (Zhou et al, 2010). The driving force for this homing is not clear yet but some chemokines and cytokines are suspected to function.

Previously our group has shown that oval cell marker FLT3, functions during the progenitor cell-dependent regeneration. The intracellular localization of the protein changes upon PH. This suggests that FLT3 could be required for the activation of the repair process (Aydin et al, 2007).

1.1.5 Liver Fibrosis

Fibrosis is the state of the tissue, where accumulated extracellular matrix proteins change the tissue architecture in response to injury. Upon hepatic injury, and the activation of the regeneration signal, hepatic stellate cells become activated and gain a myofibroblastic phenotype (Freidman, 2008). These activated myofibroblasts secrete a wide range of matrix proteins especially collagen, in order to participate the wound healing process of the liver and induce an inflammation response. Recent advances have also shown that stellate cell driven myofibroblasts are not the only source of the matrix protein secretion but portal fibroblasts and myofibroblasts from the bone marrow also participate in fibrosis. Myofibroblast activation is achieved mainly by TGF-β signaling (Gressner and Weiskirchen, 2006).

Following chronic liver injury, besides activation of stellate cells and proliferation of myofibroblasts, fibrosis leads to; accumulation of extracellular matrix proteins in between sinusoidal endothelial cells and hepatocytes, activation of Kupffer cells and infiltration of lymphocytes for inflammation response, apoptosis of the hepatocytes and an increase in resistance to blood flow through the sinusoidal endothelial cells. Finally extensive fibrosis leads to liver cirrhosis (Baraller and Brenner, 2005).

1.1.6 Cirrhosis

The clinic description of cirrhosis is the replacement of normal liver lobules with abnormal nodules separated by fibrous tissue. As liver reaches end-stage fibrosis, the diagnosis of cirrhosis can be made (Garcia-Tsao et al, 2009). Cirrhosis leads to portal hypertension and end-stage liver disease. Hallmarks of cirrhotic liver are reduced hepatocyte volume and imbalanced accumulation of extracellular matrix components, as in the case of fibrosis, but more progressive.

The foremost treatment for cirrhosis is liver transplantation. But the limitations against this treatment have urged new therapeutical approaches mainly consisting of stem cell therapies, which aim to complement the loss of hepatocytes and excessive extracellular matrix accumulation (Chen et al, 2010).

One interesting study that is aimed to show the mechanisms behind the end stage cirrhosis has revealed that the molecular markers for cirrhosis vary due to the starting reason of the disease. For example, MHC Class I C-4 subunit was found to be upregulated in cirrhotic livers caused by the Hepatitis C Virus, when compared to other cirrhotic tissues. Also many inflammation related genes were found to be upregulated in cirrhosis (McCaughan et al, 2000).

The reasons that cause cirrhosis can also result in HCC eventually. This is achieved by the gain of telomerase activation of the hepatocytes in the cirrhotic liver (Farazi and DePinho, 2006).

1.1.7 Hepatocellular Carcinoma

Major factors that lead to the development of HCC are chronic hepatitis B and C infection, excessive alcohol consumption, aflatoxin-B1 exposure and progressive cirrhosis. These risk factors have different mechanisms for hepatocellular carcinogenesis (Figure1.5) (Farazi and DePinho, 2006).

The hallmarks of liver cancers are the loss of cell cycle regulation due to mutations or genetic aberration in key regulators of cell cycle such as p53, p16, Retinoblastoma (Rb) or Cyclin D1, excessive angiogenesis due to increased vascular endothelial growth factor (VEGF), platelet derived growth factor (PDGF) signaling, increase in anti-apoptotic signals (Farazi and DePinho, 2006), TERT activation for immortality (LLovet and Bruix, 2008). In addition, copy number variations or epigenetic reprogramming are also observed in HCC (Villanueva et al, 2007).

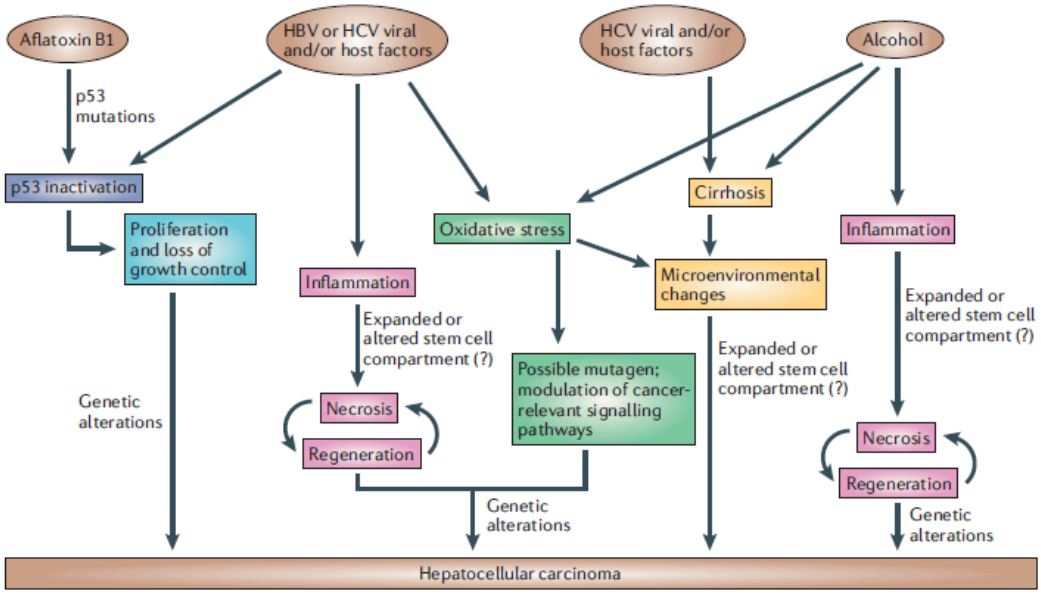

Figure 1. 5 Mechanisms for Hepatocellular carcinogenesis (Farazi and DePinho, 2006)

Finally, the involvement of cancer stem cells (CSCs) also contributes to the progression of HCC. In the case of HCC there isn't a single marker for CSC. Liver CSC can be identified by their CD133 positivity (Yin et al, 2007), OV6 (a hepatic progenitor marker) positivity (Yang et al, 2008), EpCAM and Alfa-fetaprotein double positivity (Yamashita et al, 2009), CD90 and CD45 double positivity (Yang et al, 2008) or by isolating the side population cells (Chiba et al, 2006).

1.1.7.1 Epithelial-Mesenchymal Transitions and Hepatocellular Carcinoma

Type 3 EMT is observed during tumorigenesis and is associated with increased invasiveness and metastasis of the primary tumors. The epithelial carcinoma cells acquire a mesenchymal phenotype, which is confirmed by the loss of E-Cadherin and gain of the expression of some mesenchymal markers such as α-smooth muscle actin and vimentin. These mesenchymal cells are responsible for the metastasis of the tumors. The invasion-metastasis cascade consists of intravasation, transport via circulation, extravasation at the site of metastasis, finally formation of micrometastases. Eventually secondary epithelial tumors are formed when the migrating mesenchymal cells undergo MET. The signals that derive this metastatic cells is still unclear but involvement of TGF-β, growth factor signaling via RTKs such as epidermal growth factor (EGF), and platelet derived growth factor (PDGF) and epigenetic reprogramming are well established (Kalluri and Weinberg, 2009).

Besides giving tumor cells an invasive and metastatic phenotype, recent data have also shown that the cells undergone EMT gain some stemness features. EMT in tumors not only induces metastasis but they also induce drug resistance. The intersections between the pathways involved in EMT and activated in stem cells are strong evidences for the relation between EMT and CSCs. For example in the case of CSCs of the breast cancer (CD44+CD24-/low), these metastatic cells found to be expressing TGF- β, and when TGF- β signaling is inhibited, they become epithelial like. This suggests that as TGF- β, signals involved in EMT can also be important in CSC's maintenance (Singh and Settleman, 2010).

1.2 Fms-Like Tyrosin Kinase (FLT3)

Throughout previous sections, relations between FLT3 and liver development and liver regeneration have been explained. For better understanding, in this section the FLT3 signaling will be analyzed in detail.

1.2.1 Structure of FLT3

Fms-like tyrosine kinase 3 is a type III tyrosine kinase (RTK) which is also known as fetal liver kinase-2 (FLK-2) and stem cell kinase-1 (STK-1), was first isolated as a hematopoietic stem cell marker (Matthews et al, 1991). It was shown that stem cells and progenitor cell populations expressed high FLT3 despite its absence in mature cells (Matthews et al, 1991). Human FLT3 is located on chromosome 13q12 and its mouse counterpart is located on chromosome 5, region G (Rosnet et al, 1991). The gene codes 993 amino acid length protein with 85% amino acid sequence homology between human FLT3 and mouse FLT3 (Rosnet et al, 1993). FLT3 contains five immunoglobulin like extracellular domains, a transmembrane domain, a juxtamembrane domain and two intracellular tyrosine kinase domains (TKDs) linked by a kinase insert, whose functions vary from ligand recognition, receptor activation and signal transduction (Figure 1.6). The protein exists in two forms, one is the glycosylated membrane bound form, which is 160kDa, and the other is the 130kDa protein, which is not membrane bound (Lyman et al, 1993).

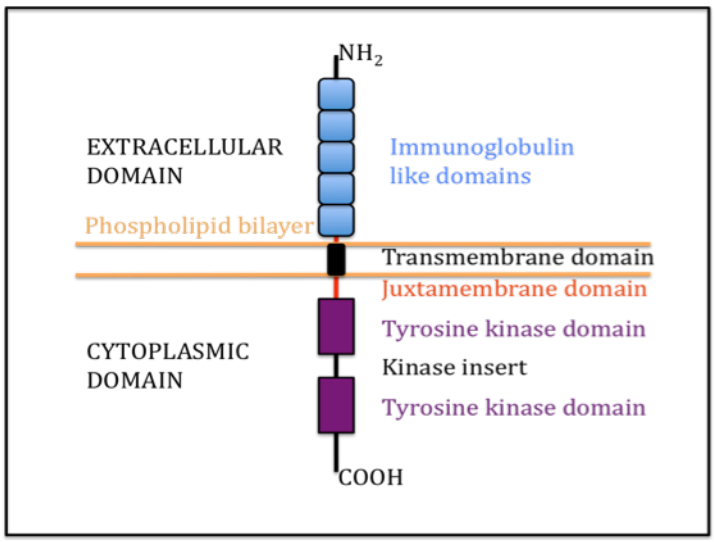

Figure 1. 6 FLT3 Structure The orientation of the protein in the phospholipid bilayer and the domains can be seen.

1.2.2 FLT3 Signal Transduction

1.2.2.1 FLT3 Ligand (FLT3L)

Activated FLT3 functions as a dimer, where its phosphlorylation is achieved via the tyrosine kinase domains. In order to form a dimer, due to the steric hindrance issues, the receptor needs to change confirmation which is enabled by ligand binding that leads to the phoshorylation and activation of the receptor. The ligand specific for FTL3 is FLT3 Ligand; FLT3-L. The chromosomal location of the gene coding the FLT3L is 19q13.3-13.4 and it codes a type I transmembrane protein, which is secreted as a soluble homodimeric protein and shown to induce proliferation of FLT3 transfected cells. Mouse FLT3L was cloned in 1993 (Lyman et al, 1993) and human counterpart was cloned in 1994 (Hannum et al, 1994). Although the expression of FLT3 is restricted to early progenitors of hematopoietic cells, thymus, lymph nodes (Rosnet et al, 1993) and placenta, brain, gonads (Maroc et al, 1993), FLT3L shows a wider range of expression in many tissues of different origins. This

suggests that the effect of FLT3 signaling is controlled by the restricted expression of FLT3 (Drexler and Quentmeier, 2004).

1.2.2.2 Activation of the Receptor and FLT3 Signaling

Suggested action mechanism of FLT3L is paracrine signaling where activation could occur through direct contact with the neighboring cells or via local secretion. The close proximity of early progenitors expressing FLT3 and the low concentration of the ligand in the normal serum samples also supported this mechanism. An autocrine feedback loop is also another scenario due to the co-expression of the receptor and the ligand (Brasel et al, 1995)

Upon ligand binding, FLT3 changes confirmation and forms a homodimer, which brings the kinase domains in close proximity for phosphorylation. After dimerization, the downstream signaling is initiated following by internalization and subsequent degradation of the complex. These processes happen very quickly where the first degraded products of the FLT3L-FLT3 complex is seen within 20 minutes after stimulation (Turner et al, 1996). Various intracellular signaling pathways are activated via the active FLT3 (Figure 1.7). Chimeric protein analysis with FMS-FLT3 RTKs has shown that FLT3 interacts SH2 domain containing proteins for phosphorylation docking sites and these sites can interact with different signaling molecules such as phophatidylinositol 3-kinase (PI3K) and growth factor receptor-bound protein 2 (Grb2; an adaptor protein). PI3Ks downstream effectors are protein kinase B (PKB/AKT), mammalian target of rapamycin (mTOR) and those of Grb2 are mitogens activated kinase (MAPK) pathway elements. Both these pathways induce transcription and translation of crucial regulatory genes involved in proliferation and block apoptosis via post-translational modifications to pro-apoptotic proteins such as BCL2 family of proteins (Stirewalt and Radich, 2003).

Similar to all forms of tyrosine kinase signaling, FLT3 signaling participates in many physiological processes through out embryogenesis and development. In addition, due to their ability to activate many downstream signaling pathways involved in cell cycle progression and prevention of apoptosis, tyrosine kinases are one of the most studied molecules for cancer therapies. Many therapeutic agents for inhibiting the kinase activity of these proteins have been identified and many more are under investigation. The high incidence of FLT3 mutations in AML and some other blood malignancies marked FLT3 as a good candidate for potential therapies against these cancer types. There are ongoing phase III trials and the combination of these with the conventional chemotherapies gives promise to the prognosis of cancer with FLT3 mutations (Sanz et al, 2009).

Also there are small molecules, which inhibit the tyrosine kinase activity of the protein such as K-252a. Phase II/III clinical trials for AML are continuing for such small molecule inhibitors of FLT3 (Cools et al, 2004).

1.2.3 Physiological Functions of FLT3

As stated earlier, FLT3 signaling is shown to stimulate the proliferation of myeloid and lymphoid progenitor cells. Besides being a hematopoietic lineage marker, FLT3 and its ligand FLT3L have some important physiological roles in the immune system by inducing dendritic cell (DC) development, which are antigen-presenting cells. DCs are generated from FLT3 expressing early myeloid or lymphoid progenitors and stimulation with FLT3L is essential for the development of DCs (Wu and Liu, 2007). FLT3-FLT3L interactions are also important for T-cell development in the thymus. Thymic recovery is maintained by FLT3L expressing perivascular fibroblasts which are in close proximity to the thymic entry site of FLT3 expressing progenitor cells for T-cell production (Kenins et al, 2010). Other than its role on immunity, FLT3 also has a role in the maintenance of neural stem cell populations. It is highly expressed in some regions of embryonic central nervous system (CNS) such as spinal cord and

dorsal root ganglia. However, contrary to its proliferative effects during embryonic development, FLT3 inhibits the neural stem cell proliferation but promotes neuronal survival, upon ligand activation with neural growth factor (NGF) (Brazel et al, 2001). These various responses of cells to FLT3 activation may be due to the various secondary signaling molecules activated and interplay of other signaling molecules in the cellular microenvironment. But which response to give still remains a mystery.

Hepatic bipotential progenitor cell (oval cell in rodents) marker FLT3, also functions in liver regeneration. In rat liver regeneration models, upon PH and 2-AAF treatment, FLT3 is expressed in hepatocytes in different time points after PH. Also in early hours after PH, FLT3 is localized in the membrane but later it changes its localization and becomes cytoplasmic (Aydin et al, 2007) which suggests that postranslational mechanisms such as translocation may play important roles in FLT3 activity during regeneration.

1.2.4 Pathophysiological Functions of FLT3

Since FLT3's proliferative and anti-apoptotic role on the cells are established, it is not surprising to observe its aberrant expression in cancers. It was first described in hematopoietic malignancies such as acute myeloid leukemia (AML), where the first mutations of FLT3 were identified. One of the first identified and mostly observed mutations is the internal tandem duplication (ITD) mutation. ITDs vary between 3 to >400 base pairs, rely in exons 14 and 15. This site corresponds to the juxtamembrane domain and tyrosine kinase domain (Nakao et al, 1996). ITDs lead to a constitutively active protein, where the ongoing proliferative and anti-apoptotic signal leads to cancer formation. It was shown that 20.4% of AML patients exhibited ITD (Thiede et al, 2002). Other than ITD, missense point mutations in exon 20 of the tyrosine kinase domain had been shown as a common mutation also. These mutations reside in the codon 835 of the gene and are associated with 7.7% of the AML patients. In addition to these

common ones, there are other mutations, which are collectively found in approx. 25-45% of AML patients (Stirewalt and Radich, 2003). Although they have smaller frequencies, many other mutations of FLT3 are also associated with different forms of leukemia other than AML.

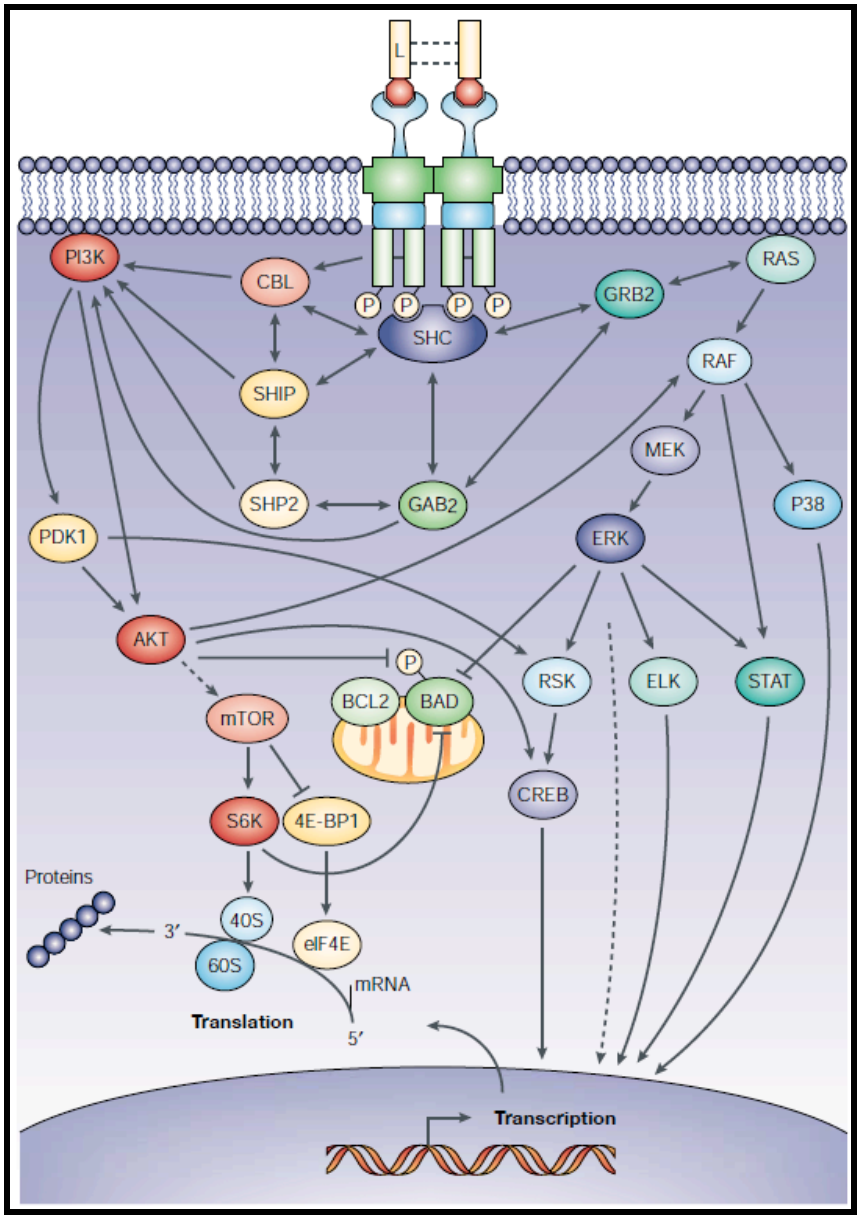

Figure 1. 7 Downstream Effectors of FLT3 (Stirewalt and Radich, 2003)

2. Aim of the Study

HCC is one of the most highly seen and lethal cancers all over the world. Lack of biomarkers for early prognosis, as well as targeted therapies and resistance to chemotherapeutic agents are some of the important reasons of its high incidence and lethality.

There are strong evidences that show a link between the disease and risk factors such as HBV, HCV infection, aflotoxins and excessive alcohol consumption. However the molecular mechanisms of the progression of HCC are not well characterized. This lack of characterization also halts the formation of good diagnostic and prognostic markers. In addition, possible links between liver regeneration and HCC are not explored in detail. The molecular signature of different stages of fibrosis, cirrhosis and HCC will reveal good candidates for diagnostic and therapeutic purposes.

Therefore we aimed to come up with a new marker for HCC, which can differentiate between different stages of the disease ranging from fibrosis to cirrhosis and cancer. Such a marker will also be helpful to predict the prognosis of the disease.

FLT3, which is a hematopoietic stem cell marker, is also an oval cell marker FLT3 and previously our group has shown its importance in liver regeneration. Also the close relation between fetal liver and hematopoiesis and the pathways activated by FLT3 made it a good candidate for analysis. Therefore, we hypothesize that FLT3 might be the link between the liver regeneration and hepatocellular carcinogenesis. By investigating the function of FLT3 *in vitro* and *in vivo* hepatocellular carcinoma models, we aimed to show its role in hepatocellular carcinogenesis.

3. Materials and Methods

3.1 Cell Culture

14 different HCC (Hep3B, HepG2 Hep40, Huh7, PLC/PRF/5, Mahlavu, Sk-Hep1, Focus, Snu182, Snu387, Snu398, Snu423, Snu449 and Snu475) cell lines and HEK293 cell lines were used during this study. Hep3B, HepG2 Hep40, Huh7, PLC/PRF/5, Mahlavu, Sk-Hep1 and Focus cell lines were cultured in Low-glucose DMEM. Snu182, Snu387, Snu398, Snu423, Snu449 and Snu475 were cultured in RPMI1640 (HyClone, Utah, USA) Both media were supplemented with 10%FBS, 100U/ml penicillin-streptomycin and 0.1mM non-essential amino acids (HyClone, Utah, USA). Cells were incubated at 37°C with 5% CO_2 and media were changed every 3 days. For cryopreservation 90% FBS, 10% DMSO mixture was used for freezing medium and cells were stored at -80°C for several months or at liquid nitrogen storage tank for longer periods of time.

3.1.1 K-252a Treatment of HCC cell lines

FLT3 inhibitior (K-252a Nocardiopsis sp., Calbiochem) was added to the culturing media of Snu182, Snu398, Huh7 and Hep40 cell lines at 200nM concentration and treated for 2 hours prior to further experiments. As control group, these cells were cultured for 2 hours with same volume of DMSO.

3.2 Nude-Mice Tumor Xenografts

Snu182, Snu398, Huh7 and Hep40 cells that were either treated with K-252a or DMSO (as explained in section 3.1.1) were tyrpsinated and then pelleted at 1500rpm for 5 minutes, washed with 1xPBS, counted and re-pelleted. Final pellets were dissolved in 1xPBS and aliquoted at a concentration of $6x10^6$ cells/250μL. For each group, 5 nine-month-old male nude mice (CD1) were used. In order to eliminate differences in each animal, cells treated with inhibitor were

subcutaneously injected to the right side of the animals whereas control cells were injected to the left side of the animal. Tumor sizes were measured on regular periods. Significance of the differences in tumor sizes was calculated with student's t-test. The animals were housed under controlled environmental conditions (22ºC) with a 12-hour light and 12 hour dark cycle in the animal holding facility of the Department of Molecular Biology and Genetics at the Bilkent University. This study protocol complied with Bilkent University Local Ethic Committee (BILHADYEK) guidelines on humane care and use of laboratory animals. The animals were permitted unlimited access to food and water at all times.

3.3 Standard Buffers and Solutions

Ingredients of the standard solutions and buffers mentioned throughout the Materials and Methods section is given in Section 6. Appendix.

3.4 Total RNA Isolation

When the cells were more than 80% confluent, they were trypsinated at 37°C for 3-5 minutes. Then trypsin was inhibited with fresh media (DMEM or RPMI depending on the cell line) and cells were pelleted at 1500rpm for 5 minutes. Pellet was re-suspended with 1xPBS and pelleted again. RNA isolation was performed by RNeasy Midi Kit (QIAGEN, Hilden, GERMANY) according to the manufacturer's protocol. The concentrations and the OD_{260} and OD_{280} values of the RNA samples were measured by NanoDrop ND-1000 (NanoDrop Technologies, USA). RNA denaturating gel electrophoresis was performed to check the integrity of the RNAs and presence of DNA contamination.

3.5 cDNA Synthesis

cDNAs were synthesized from the isolated total RNA samples by using DyNAmo cDNA Synthesis Kit (Finnzymes, FINLAND). 2µg RNA was used for each reaction with a total volume of 40µL. RNA was diluted with DEPC-ddH_2O with a total volume of 14µL, then 2µL of oligodT primer was added. This mixture was incubated at 65°C for 5 minutes and chilled on ice for 3-5 minutes. Then 20µL 2X Reverse Transcriptase Reaction Buffer and 4µL M-MulV RT RnaseH enzyme was added to each reaction. Conditions for cDNA synthesis were 25°C for 10 minutes, 45°C for 45 minutes and 85°C for 5 minutes.

3.6 Reverse Transcriptase-Polymerase Chain Reaction (RT-PCR)

Primers were designed by using the online Primer3 tool v.0.4.0 (http://frodo.wi.mit.edu/primer3/) and NCBI primer BLAST tool (http://www.ncbi.nlm.nih.gov/tools/primer-blast/). The list of the primers used during this study is shown on Table 3.1.

Table 3. 1 Primers used for expression analysis in RT-PCR

Gene Name	Product Size	Forward Primer (5'-3')	Reverse Primer (5'-3')	Tm (°C)
FLT3 set 1	114 bp	GGAAGAAGAGGAGGACTTA	AGGTCTCTGTGAACACACGA	60
FLT3 set 2	184	ATGGATTCGGGCTCACCT	GCTGATTGACTGGGATGC	60
CD133	183	AATGACCCTCTGTGCTTGGT	GGATTGATAGCCCTGTTGGA	60
CD34	187	GGCCACAACAAACATCACAG	AACATTTCCAGGTGACAGGC	60
CD90	124	TGACCCGTGAGACAAAGAAG	GTGAAGGCGGATAAGTAGAG	60
CD45	217	TTGGCTTTGCCTTTCTGGAC	TGGGTGGAAGTATTGTCTGG	60
LGR5	195	GGAGCATTCACTGGCCTTTA	ATTGTCATCCAGCCACAGGT	60
E-cadherin	119	GACTCGTAACGACGTTGCAC	GGTCAGTATCAGCCGCTTTC	60
Vimentin	110	GCAGGAGGAGATGCTTCAGA	ATTCCACTTTGCGTTCAAGG	60
Fibronectin	108	AATATCTCGGTGCCATTTGC	CAGTAGTGCCTTCGGGACTG	60
α-SMA	165	TATCAGGGGGCACCACTATG	GCTGGAAGGTGGACAGAGAG	60
Sip1/ZEB2	132	TGTAGATGGTCCAGAAGAAATGAA	TTGGCAAAGTATTCCTCAAAATCT	60
GAPDH multiplex	611	AGTCAACGGATTTGGTCGTATT	GTAGAGGCAGGGATGATGTTCT	60
GAPDH	119	GGCTGAGAACGGGAAGCTTGTCAT	CAGCCTTCTCCATGGTGGTGAAGA	60

The reaction mixture that was used in RT-PCR analysis is shown in table 3.2. Buffers and enzymes were supplied from Finnzymes, FINLAND.

Table 3. 2 Reaction mixture for RT-PCR

Ingredient	**Volume** (μL)
cDNA	1
10x Taq Reaction Buffer	2.5
10mM dNTP	0.5
50mM $MgCl_2$	0.75
Forward Primer (10pmol)	1
Reverse Primer (10pmol)	1
Taq Polymerase (1U)	0.5
ddH_2O	17.75
Total	**25**

RT-PCR was performed with the following conditions for all of the primers except GAPDH, for GAPDH, reaction was performed for 23 cycles;

Initial denaturation: 95°C 5 minutes

94°C 30 sec
60°C 30 sec **30 cycles**
72°C 30 sec

Final extension: 72°C 5 minutes

3.6.1 Multiplex PCR for Sip1/Zeb2 and GAPDH

The reaction mixture that was used in Multiplex PCR analysis is shown in table 3.3.

Table 3. 3 Reaction mixture of Sip1-Gapdh multiplex RT-PCR

Ingredients	**Volume (μL)**
cDNA	1
10x Reaction Buffer	2.5
10mM dNTP	0.6
50mM $MgCl_2$	0.75
Sip1 Forward primer (10 pmol)	2
Sip1 Reverse primer (10 pmol)	2
Gapdh Forward primer (10pmol)	0.15
Gapdh Reverse primer (10pmol)	0.15
Taq Polymerase	0.5
dd-H_2O	15.35

The following conditions were used for the reaction.

Initial denaturation: 95°C 5 minutes

94°C	30 sec		
60°C	30	sec	**35 cycles**
72°C	30 sec		

Final extension: 72°C 5 minutes

3.6.2 Agarose Gel Electrophoresis

1.5% agarose gel was prepared with 1XTAE Buffer and ethidium bromide (30ng/mL). Samples were prepared with 6X Agarose Gel Loading Dye (1X in final mixture) and loaded on gel, which ran at 120V for 25 minutes. Visualization was performed by Transilluminator (Vilber Lourmat, FRANCE) and photos were taken with ChemiCap software. As a marker, Gene Ruler DNA Ladder Mix (MBI Fermantas, Ontario, CANADA) was used.

3.7 Protein Isolation

3.7.1 Total Protein Isolation

Cells were scraped in 1XPBS and pelleted after centrifugation at 1500 rpm for 5 minutes in order to preserve the extracellular proteins. Total protein isolation was performed by re-suspending the pellet in Lysis Buffer (Appendix), whose amount depends on the size of the pellet (approx. 200 μL). The pellet was homogenized and incubated on ice with occasional vortexing for complete lysis. Then the cell lysate was centrifuged at 13.000 rpm for 20 minutes at +4°C. Supernatants were collected and protein concentration was measured with Bradford Assay.

3.7.2 Protein Quantification with Bradford Assay

Standard curve for Bradford Assay was performed with different concentrations of Bovine Serum Albumin (Sigma, Montana, USA). As blank for samples, lysis buffer was used. OD was measured at 595nm wavelength, with Beckman DU 640 Spectrophotometer and concentrations were calculated according to the standard curve obtained for BSA results. Table 3.4 shows the preparation of the standard curve. Protein samples with unknown concentrations were prepared as 2µL protein, 98µL ddH20 and 900µL Bradford Reagent.

3.8 Western Blotting

3.8.1 SDS-Polyacrylamide Gel Electrophoresis (SDS-PAGE)

Depending on the size of the protein to be analyzed, different concentrations of resolution gel (10% (for proteins in the range of 40 and 90kDa) and 7.5% (for proteins larger than 90 kDa)) and 5% stacking gels were prepared. 25µL of 30µg protein was loaded to the gels. Proteins samples were prepared with cracking buffer, by denaturating at 90°C for 5 minutes. Two different types of prestained protein markers were used. For proteins with higher molecular size, Fermantas Spectra Multicolor Broad Range Protein Ladder (MBI Fermantas, Ontario, CANADA) and for smaller proteins, Fermantas PageRuler Prestained Protein Ladder (MBI Fermantas, Ontario, CANADA) was used. Gels were run at 80-120V with cold 1X Running Buffer. Before transfer, stacking gel was removed and gel was gently washed with ddH_2O. Then it was put into transfer buffer. The size of the protein also determined the type of the transfer that needed to be performed.

Table 3. 4 BSA standard curve for Bradford Assay

BSA standard	***1(µL)***	***2(µL)***	***3(µL)***	***4(µL)***	***5(µL)***	***6(µL)***	***7(µL)***	***8(µL)***	***9(µL)***	***10(µL)***
BSA (1µg/µL)	0	2.5	5	7.5	10	12.5	15	20	25	35
ddH_2O	100	97.5	95	92.5	90	87.5	85	80	75	65
Bradford Reagent	900	900	900	900	900	900	900	900	900	900

3.8.2 Transfer of Proteins to the PVDF Membrane

Four whatman papers and PVDF Transfer Membrane (0.45µm, Thermo Scientific, USA) were cut at the size of the gel and membrane was treated with methanol for 30 seconds and ddH2O for 2 minutes.

3.8.2.1 Semi-Dry Transfer For Proteins around 40-100kDa

Two whatman papers, membrane, gel and two more whatman papers were carefully aligned in BioRad Semi-Dry transfer apparatus (Bio-Rad, California, USA). Transfer was performed at a constant current, with 3.5mA for 1 cm^2 of the membrane for 45 minutes. Then the gel was moved into Commasie Solution for detecting the efficiency of the transfer for 30 minutes and then destained. Membrane was put into 1X TBS-T (01%) for 5 minutes.

3.8.2.2 Wet Transfer for Proteins with molecular weight larger than 100kDa

Two whatmans, membrane, gel and two more whatmans were aligned in between sponges of BioRad gel tank (Bio-Rad, California, USA) and soaked into Wet Transfer buffer. Overnight transfer was performed at 16 V at 4°C. Then the gel was moved to Commasie Solution for detecting the efficiency of the transfer for 30 minutes and then destained. Membrane was put into 1X TBS-T (01%) for 5 minutes.

3.8.3 Immunological Detection of Immobilized Proteins

Blocking of the membrane was performed for 2-4 hours in non-fat dry milk powder block. Then the membrane was incubated overnight with primary antibody at 4°C. Primary antibodies and the conditions that were used for western blotting studies are shown in table 3.5. The membrane was gently rotated on a shaker during these steps.

Table 3. 5 Antibodies used for Western Blotting analysis.

Protein Name	**Brand**	**Catalog no.**	**Incubation time and temperature** (°C)	**Source**	**Molecular Weight (kDa)**	**Antibody concentration used**
FLT3	Cell Signaling Technology	3462	o/n at +4	Rabbit (mAb*)	130-160	1/1000 in 5%BSA block
Calnexin	SantaCruz Biotechnologies	sc-6465	o/n at +4	Goat (pAb**)	90	1/1000 in 5%non-fat dry milk block

(*mAb: monoclonal antibody, **pAb: polyclonal antibody, o/n: over night)

After primary antibody incubation, membrane was washed three times with TBS-T (1%) for 10 minutes. Secondary antibody incubation was performed at RT for one hour. HRP-linked secondary antibodies and the conditions that were used during western blotting are shown in table 3.6. Secondary antibodies were also prepared in 5% non-fat dry milk block.

Table 3. 6 Secondary Antibodies used in Western Blotting

Antibody	**Brand**	**Catalog no.**	**Dilution Factor**
Anti-Rabbit IgG	Cell Signaling Technology	7074	1/2000
Anti-mouse IgG	SantaCruz Biotechnologies	sc-2318	1/2500
Anti-goat IgG	SantaCruz Biotechnologies	sc-2033	1/5000

After secondary antibody incubations, membrane was washed three times with TBS-T (0.1%) for 10 minutes. The membrane was then treated with SuperSignal West Femto Maximum Sensitivity Substrate (Thermo Scientific, USA), as stated in manufacturer's protocol. Then membrane was placed on a glass, covered with stretch film and placed in film cassette (Amersham Life Sciences, New Jersey, USA). Film was developed with Hyperprocessor (Amercham Life Sciences, New Jersey, USA).

3.9 Immunostaining procedures

For immunostaining procedures, anti-FLT3 antibody (sc-340, SantaCruz Biotechnologies, California, USA) was used at 1/200 concentration in blocking solution.

3.9.1 Immunohistochemistry Staining for Paraffin Embedded Tissue Sections

Paraffin embedded tissue sections were de-parafinized in xylene for 15 minutes. Sections were then treated with decreasing concentrations of EtOH for hydration and washed with ddH2O. Antigen retrieval was performed in sodium citrate buffer for 10 minutes at 90°C. Then slides were cooled to RT and washed with PBS-T (0.1%). After 30 minutes of 3% H2O2 incubation and washing with PBS-T, one hour blocking was performed in a humidified chamber. Primary antibody (FLT3 in 1/200 dilution) incubation was performed overnight at +4°C. After washing once more with PBS-T, slides were treated with Biotin-link Anti-mouse & Anti-Rabbit IgG (DakoCytomation, Glostrup, Denmark) and with Streptavidin-HRP red solution (DakoCytomation, Glostrup, Denmark) for 30 minutes respectively. Slides were washed with PBS-T and were incubated with DAB+Chromogen Substrate (DakoCytomation, Glostrup, Denmark) until the staining was observed (2-5 minutes). To stop the color development, tap water was applied to the slides. For counter staining, they were dipped in to

hematoxylene for 1 minute, and again washed with tap water. Specimens were mounted with Faramount Aqueous Mounting Medium (DakoCytomation, Glostrup, Denmark), with coverslips (Deckglaser 100 no.1 12mm). The photos were taken with light microscope Leica TCS/SP5, Japan.

3.9.2 Immunoflourescense Staining for Frozen Tissue Sections

Frozen sections were fixed with 4% paraformaldeyde for 30 minutes and then washed with PBS-T (0.1%). After 30 minutes of 3% H_2O_2 incubation and washing with PBS-T, one hour blocking was performed in a humidified chamber. Primary antibody (FLT3 in 1/200 dilution) incubation was performed overnight at +4°C. After washing once more with PBS-T, slides were treated with 1/200 FITC-tagged anti-Rabbit IgG (Sigma, Montana, USA) for one hour at RT in dark. Specimens were mounted with UltraCruz mounting medium with DAPI (SantaCruz Biotechnologies, California, USA) for counter staining. Slides were observed in fluorescent microscopy (Leica TCS/SP5, Japan). Excitation wavelength for FITC and DAPI was at 490nm and at 359nm respectively.

3.9.3 Immunoflourescense Staining

Cells were grown on coverslips prior to staining. When they were approximately 80% confluent, medium was removed and washed with 1X PBS. The cells were fixed with cold methanol for 15 minutes. After washing with PBS-T (0.1%), 10 minutes of 3% H_2O_2 incubation was performed. After washing with PBS-T, coverslips were covered with blocking solution and incubated for one hour at RT. Primary antibody (FLT3 in 1/200 dilution) incubation was performed at RT for one hour. FITC-tagged anti rabbit IgG (SantCruz Biotechnologies, California, USA) was used as secondary antibody at a concentration of 1/200 dilution in blocking solution. The incubation was performed in dark for one hour at RT. Coverslips were mounted with UltraCruz mounting medium with DAPI (SantaCruz Biotechnologies, California, USA) for counter staining. Slides were

observed in fluorescent microscopy (Leica TCS/SP5, Japan). Excitation wavelength for FITC and DAPI was at 490nm and at 359nm respectively.

3.10 Wound Healing Assay

Cells were seeded on 6-well plates, in ~80% confluency. When cells were 100% confluent, 3 vertical scratches were made with a standard 200μL micropipette tip. For convenience, 2 vertical lines were drawn with marker in order to take photos of the same region each time. After the scratches were made, medium was changed either with medium containing 10% FBS or 2% to mimic serum starvation and 200nM K-252a treatment is performed for two hours or two days. For 0 hour groups, photos were taken immediately. When two-hour inhibitor incubation completed, fresh medium (either with 10% FBS or 2% FBS) was added. Mediums of samples, which undergo two-day inhibitor treatment, were not changed. Equal volume of DMSO was used in control groups. Wounds were monitored for 48 hours and photos of the same regions were taken with 24-hour intervals. The healed wound distance was measured by calculating the difference between the initial and final wound size and dividing it by 2. Measurements were taken from 10 different points and significance was calculated with student's t-test among inhibitor treated and control groups for both normal medium conditions and serum starvation conditions separately.

3.11 TUNEL Assay

TdT- (terminal deoxynucleotidyl transferase) mediated fluorescein-dUTP labeling kit (Roche Diagnostics, Mannheim, Germany) was used to detect DNA fragmentation. Cells seeded on coverslips were treated with K-252a for two hours. DMSO is used for control groups. Then cells were washed with 1XPBS and fixed with freshly prepared 4% paraformaldehyde, for one hour at RT. After washing with 1xPBS for three times, cells were treated with freshly prepared and cooled permeabilisation (0.1%Triton X-100, 0.1% sodium citrate) solution for two

minutes on ice. Then cells were washed with 1XPBS again and 30μL TUNEL Reaction mixture was added and incubated at 37°C in dark in a humidified chamber for one hour. Coverslips were mounted with UltraCruz mounting medium with DAPI (SantaCruz Biotechnologies, California, USA) for counter staining. Slides were observed in fluorescent microscopy (Leica TCS/SP5, Japan). Excitation wavelength for FITC and DAPI was at 490nm and at 359nm respectively. As negative control slides were incubated in the absence of terminal deoxynucleotidyl transferase. As positive control, 10 minutes of DNaseI (Fermantas, Ontarino, CANADA) treatment is performed at RT, prior to the incubation with TUNEL reaction mixture.

3.12 Senescence Associated β-Gal Assay (SABG)

50% confluent cells were treated with K-252a for two hours before fixation. Control groups were treated with equal amount of DMSO. Then cells were washed with 1XPBS and fixed with freshly prepared 4%paraformaldehyde for 15 minutes. After washing with 1XPBS, cells were incubated with freshly prepared and filtered SABG solution (Table 3.7), whose pH was adjusted to 6.0 with Na-P Buffer (Table 3.8) for 18 hours in dark at 37°C. After the incubation, cells were washed twice with 1XPBS and fixed with cold methanol for 5 minutes. As a counter stain, nuclear fast red was used for 5 minutes. Cover slips were washed with ddH_2O and closed with DAKO mounting medium (DakoCytomation, Glostrup, Denmark). The photos were taken with light microscope Leica TCS/SP5, Japan.

Table 3. 7 Preparation of SABG Solution

Stock Solution	For 3mL of SABG Solution (µL)
200 mM Citric Acid (pH:6.0)	600
Na-P Buffer (pH:6.0)	600
100mM Potassium Ferrocyanide	150
100mM Potassium Ferricyanide	150
2M NaCl	225
100mM $MgCl_2$	60
40mg/ml X-gal	75
ddH_2O	1140

Table 3. 8 Preparation of Na-P Buffer (pH: 6.0, Total Volume: 40mL)

1M Na_2HPO_4	10.2mL
1M NaH_2PO_4	29.8mL

3.13 Statistical Analysis

Student's t-test from Microsoft Excel 2008 for Mac (Version 12.1.0) is used. T-test is performed between inhibitor treated groups and control groups for wound healing assay (Section 3.10), TUNEL assay (Section 3.11) and nude mice xenograft's tumor sizes (Section 3.2). Significance threshold is set to 0.05, for p-value. P-values larger than 0.05 are indicated as non-significant (NS).

4. Results

We used both *in vitro* and *in vivo* models to reach our specific aim, which is to show the role of FLT3 in hepatocellular carcinogenesis. Firstly *in vitro*, we used 14 established HCC cell lines, and characterized these cells lines with FLT3 and other adult stem cell, cancer stem cell, hematopoietic stem cell markers and epithelial and mesenchymal lineage markers. Then according to their FLT3 expression levels, we chose 4 different cell lines and continued our functional studies to investigate the role of FLT3. For this purpose we used an FLT3 phosphorylation inhibitor, K-252a to inhibit its function and tested some parameters such as cellular morphologies, subcellular localization of FLT3, in vitro invasion, change in the expression of epithelial and mesenchymal lineage markers and change in their apoptotic cell numbers and induction of senescence. Then to further understand FLT3's involvement in tumorigenesis, we used nude mice xenograft models.

4.1 Characterization of HCC Cell Lines

We examined the expression profile of FLT3 as well as a panel of adult stem cell, cancer stem cell, hematopoietic lineage markers and EMT markers at our HCC cell lines. These cell lines were either well differentiated (WD) or poor differentiated (PD) HCCs. WD HCCs (HepG2, Hep3B, Hep40, HUH7 and PLC) resemble highly of differentiated hepatocytes, on the other hand PD HCCs (Mahlavu, Focus, SK-Hep-1, Snu182, Snu387, Snu398, Snu423, Snu449 and Snu475) show characteristics of non-differentiated cells (Qin and Tang, 2002).

4.1.1 Expression Pattern of FLT3 in HCC Cell Lines

We checked the expression of FLT3 at the transcript level in 14 HCC cell lines by using RT-PCR. Among them, we found that FLT3 mRNA is expressed in Hep40, Snu182 and Snu398 cell lines (Figure 4.1). Hep40 is a well-differentiated

HCC, whereas Snu182 and Snu398 cell lines are poor differentiated HCC. We used GAPDH as loading control. No expression is observed in negative control.

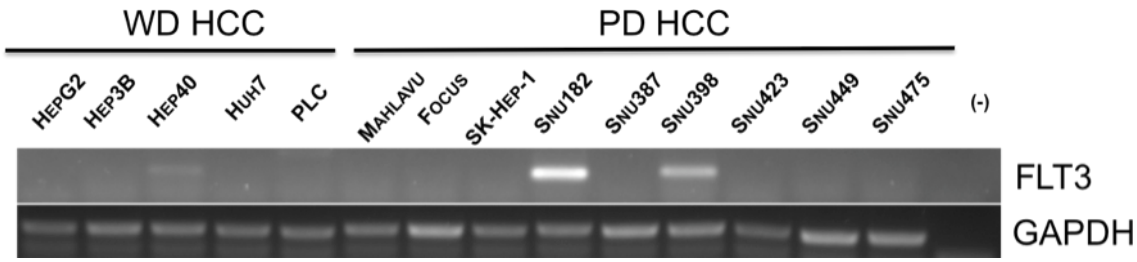

Figure 4. 1 Expression Profiling of FLT3 with RT-PCR

We performed western blot analysis in order to analyze the FLT3 protein in HCC cell lines. We found 130kDa non-glycosylated form of the FLT3 protein expression in WD HCCs Hep3B, Hep40, and PD HCCs Focus, SK-Hep1, Snu182, Snu387 and Snu398 (Figure 4.2). We used Calnexin for loading control.

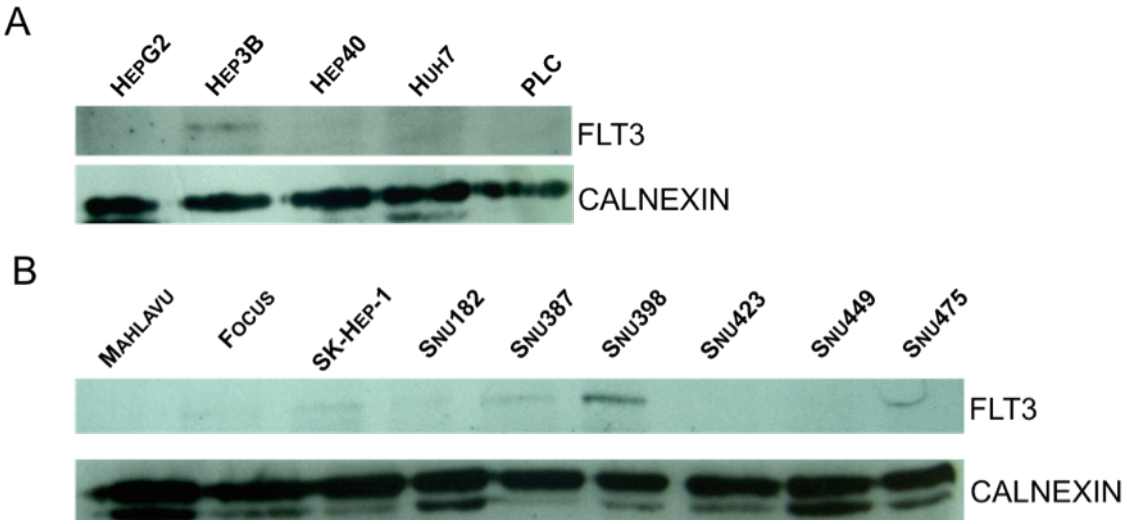

Figure 4. 2 Western blotting analysis with FLT3 antibody of (A) WD HCC cell lines and (B) PD HCC cell lines. Calnexin is used as loading control (WD: well differentiated, PD: poor differentiated).

4.1.2 Expression Analysis of Adult Stem Cell, Cancer Stem Cell and Hematopoietic Lineage Markers in 14 HCC Cell Lines

In order to assess stemness features of 14 HCC cell lines, we performed RT-PCR analysis for the markers of adult stem cell (CD90, LGR5), cancer stem cell (CD133) and hematopoietic lineage (CD34, CD45) markers. (Figure 4.3)

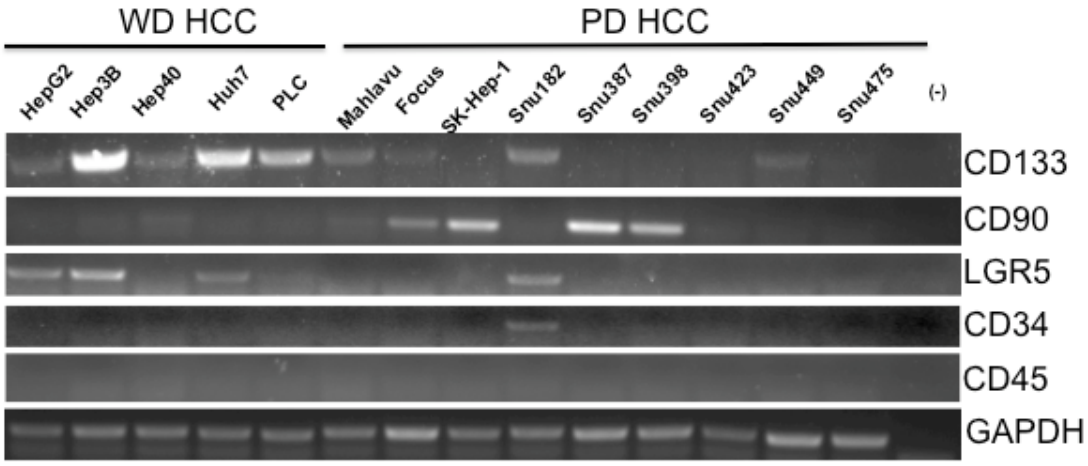

Figure 4. 3 Expression Profiling of 14 HCC cell lines for adult stem cell, cancer stem cell and hematopoietic cell lineage markers.

Our expression analysis has shown that CD133, an hematopoietic progenitor marker, which was recently associated with cancer stem cells (Gupta et al, 2009) was expressed in mainly WD HCC cell lines (HepG2, Hep3B, Hep40, Huh7 and PLC) and some of the PD HCC cell lines (Mahlavu, Focus, Snu182, Snu449). On the other hand, CD90 positivity mainly observed in PD HCC cell lines (Focus, SK-Hep-1, Snu387 and Snu398). Lgr5 showed a similar pattern with CD133. It was expressed in WD HCCs (HepG2, Hep3B, Huh7) and PD HCC Snu182. Finally when the expression of hematopoietic lineage markers expressions were analyzed via RT-PCR, it was observed that all of the HCC cell lines were negative for CD45, and only Snu182 was positive for CD34. We used GAPDH as loading control. No expression was observed in negative control.

4.1.3 Expression Analysis of Epithelial and Mesenchymal Lineage Markers in 14 HCC Cell Lines with RT-PCR

In order to investigate to which lineage does these HCC cell lines belong, we analyzed 4 different markers for EMT (Figure 4.4). E-cadherin was used as epithelial marker and Fibronectin, Vimentin and α-SMA were used as mesenchymal markers. The expressions levels of vimentin and α-SMA did not reveal any significant difference between 14 HCC cell lines, but expression of E-cad was restricted to mainly well WD HCC cell lines and Snu182. On the other hand, all the cell lines expressed Fibronectin, although its levels were variable highly, especially between Snu182 and Snu398. We used GAPDH as loading control. No expression was observed in negative control.

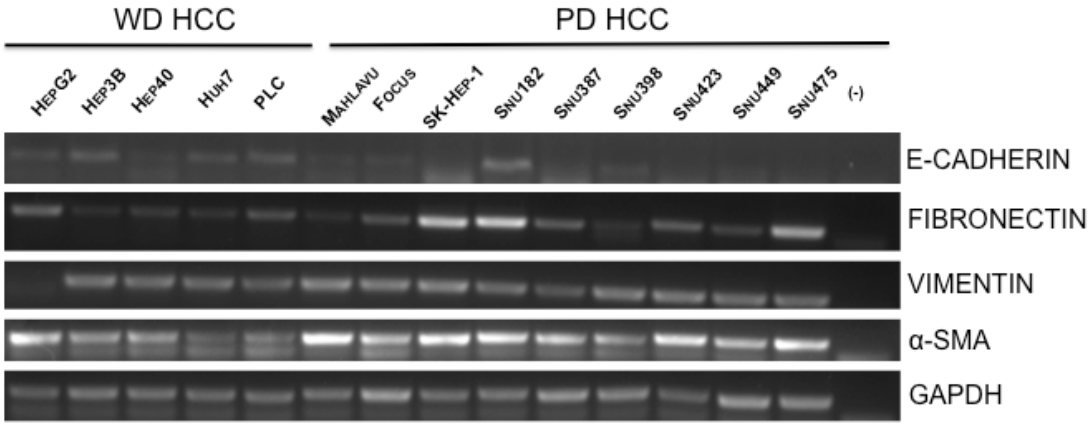

Figure 4. 4 RT-PCR analysis for Epithelial and Mesenchymal lineage markers.

4.2 Expression of FLT3 in Cirrhotic and Normal Human Liver

We examined the FLT3 expression in normal (Figure 4.5) and cirrhotic (Figure 4.6) liver samples by immunohistochemistry. Our results revealed different staining patterns in normal and cirrhotic livers.

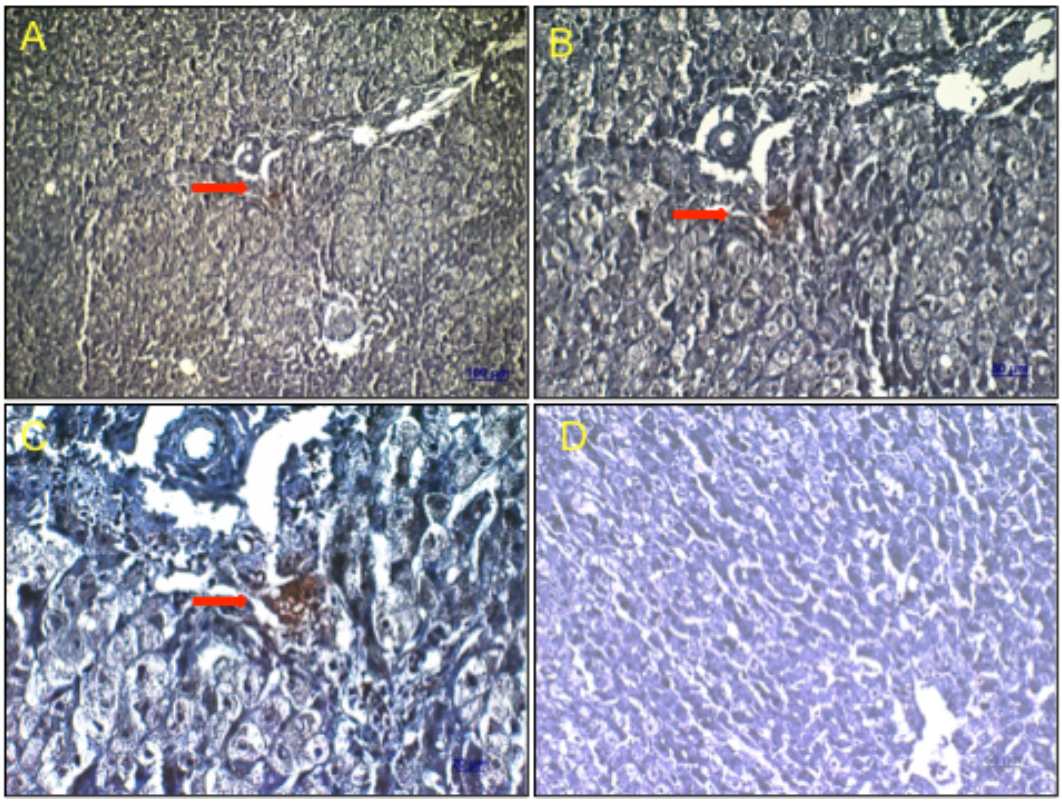

Figure 4. 5 FLT3 Immunohistochemistry of a normal liver. A, B and C are taken with different magnifications, 10x, 20x and 40x respectively. D is the negative control. (Arrowheads showed FLT3 positive cells)

In normal liver, FLT3 positivity was restricted to the cells neighboring the ductal structure. The staining observed was cytosolic (Figure 4.5A-C). In addition no staining was observed in the hepatocytes. (Figure 4.5A-C) Adversely in cirrhotic liver, there was extensive FLT3 staining in hepatocytes, giving a patchy appearance (Figure 4.6A-C). FLT3 positivity was found to be mainly cytoplasmic. No staining was observed in negative controls (Figure 4.5D and 4.6D)

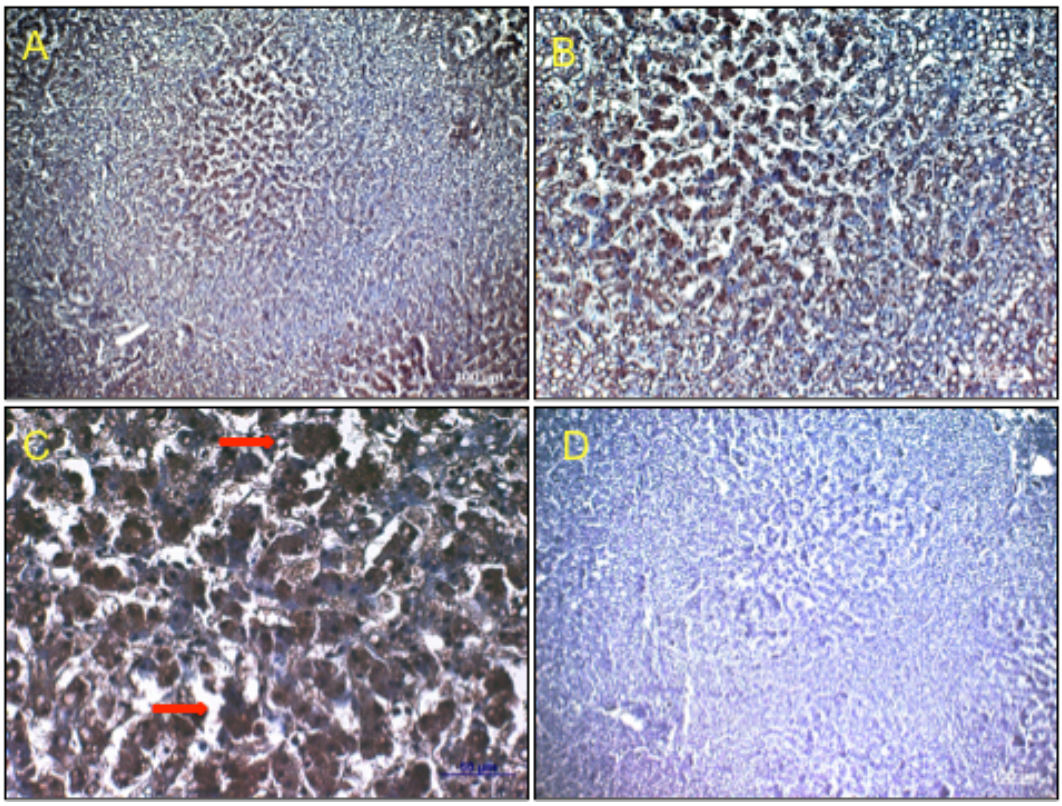

Figure 4. 6 FLT3 Immunohistochemistry of a cirrhotic liver. A, B and C are taken with different magnifications, 10x, 20x and 40x respectively. D is the negative control (Arrow heads show some of the positive staining in cirrhotic liver).

4.3 Functional Analysis of FLT3 in HCCs by Inhibiting the Phosphorylation of the Protein with K-252a

As a tyrosine kinase, FLT3 has been shown to actively participate in a wide variety of cellular events such as proliferation and block of apoptosis (Stirewalt and Radich, 2003). In this part of my thesis we aimed to investigate the function of FLT3 in HCCs. To accomplish this task, we compared the response of the cell lines Snu182, Snu398, Huh7, Hep40 before and after treating the cells with FLT3 inhibitor, K-252a, which inhibits its phosphorylation. We decided to use Snu182, Snu398, Huh7 and Hep40, because they expressed FLT3 in different levels (Figure 4.1 and Figure 4.2).

4.3.1. Effect of K-252a on the cellular morphology in HCCs

After cells reached 90% confluency, Snu182, Snu398, Huh7 and Hep40 were treated with 200nM K-252a for two hours. Upon inhibitor treatment, no significant change was observed in their morphologies of Snu182 (Figure 4.7A-B), Snu398 (Figure 4.7C-D), Huh7 and Hep40 (data not shown).

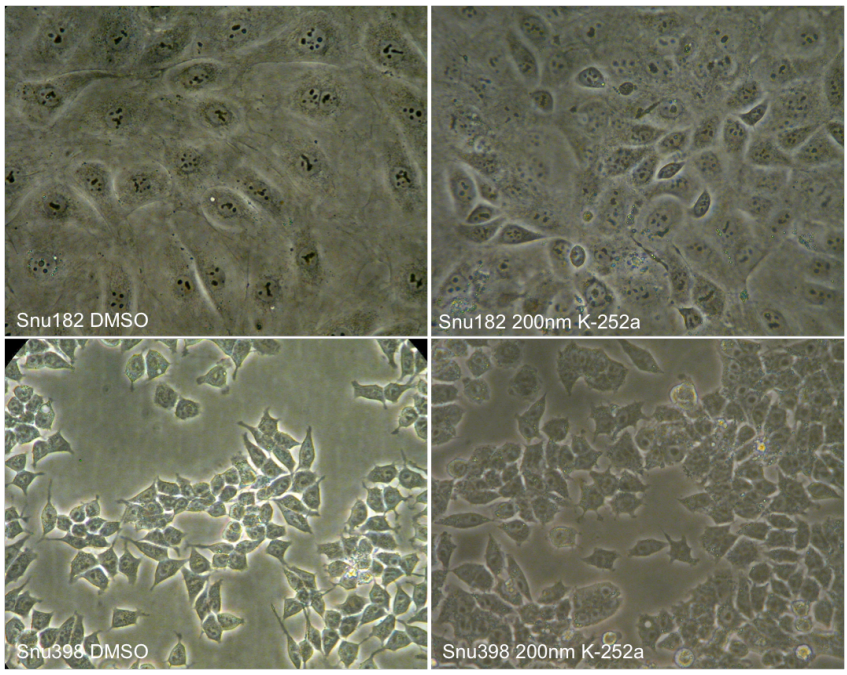

Figure 4. 7 Inverted microscopy photos of Snu182 and Snu398 after 200nM inhibitor treatment for two hours. (Magnification: 40x)

4.3.2 Effect of K-252a on the Subcellular Localization of FLT3 in HCCs

Since the previous data on liver regeneration showed that, FLT3 changed its cellular localization from membrane bound to cytosolic when subjected to PH (Aydin et al, 2007), we decided to check the subcellular localization of Snu182, Snu398, Huh7 and Hep40, in the presence and absence of FLT3 inhibitor.

We seeded Snu182, Snu398 Huh7 and Hep40 cells on glass coverslips and, treated with 200nM K-252a for two hours prior to fixation. We analyzed

FLT3 protein localization with immunofluoroscence before and after the treatment with K-252a (Figure 4.8). Our results revealed a drastic change in the localization of FLT3 in Snu182 (Figure 4.8A,B), Snu398 (Figure 4.8D,E) and Hep40 cell lines (Figure 4.8G,H) and to a lesser degree in Huh7 cells (Figure 4.8J,K). Upon inhibitor treatment, FLT3 protein was accumulated in the mainly in the nucleus and in the endoplasmic reticulum compared to cyoplasmic localization without treatment. No staining was observed in negative controls (Figure 4.8C, F, I, L).

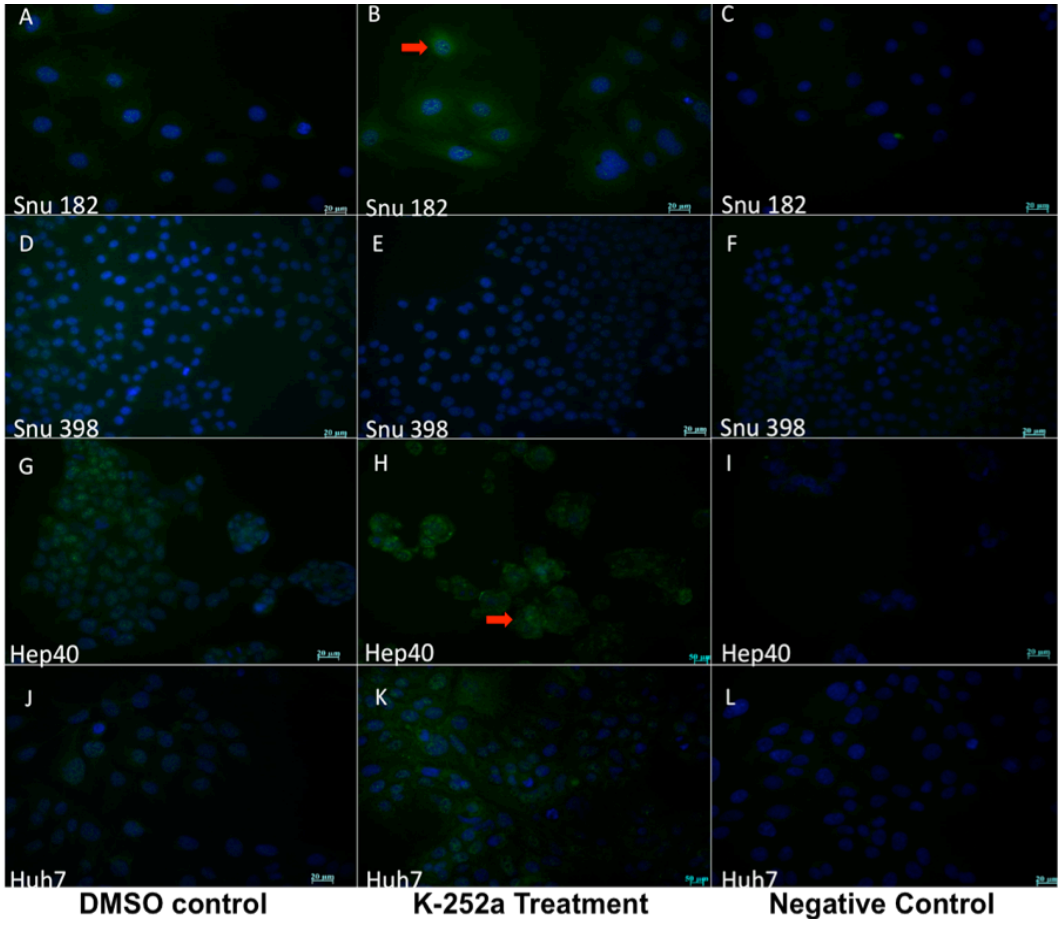

Figure 4. 8 FLT3 Immunoflouroscence Snu 182 (A-C), Snu 398 (D-E), Hep40 (G-I) and Huh7 (J-K) in the absence (A, D, G, J) and in the presence of 200nM FLT3 tyrosine kinase inhibitor K-252a Nocardiopsis sp. (B, E, H, K). Cells were treated with the inhibitor for 2 hours. Primary Ab was not used in negative controls (C, F, I, L). Nuclei were stained with DAPI. (Red arrows point the protein accumulation in the nucleus.)

4.3.3 Wound Healing Assay

The wound healing ability of cells reflects their invasion capacities. Therefore, we performed wound healing assay for Snu182 (Figure 4.9 and 4.10), Snu398 (Figure 4.11 and 4.12), and Huh7 (Figure 4.13 and 4.14), in the presence and absence of FLT3 inhibitor K-252a, both in normal medium conditions (10% FBS) and serum starvation (2% FBS). We were not able to perform this assay in Hep40 due to lack of their single cell layer growth. The photographs of the cells were taken after with 24-hour periods for 48 hours and the relative healed distance is measured from the photographs, which were taken with the same magnification each time (Figure 4.9, Figure 4.11 and Figure 4.13). Our results showed that Snu182 and Snu398 showed decreased wound healing capacity upon two-hour or two-day inhibitor treatment under both normal and serum starved conditions. Huh7, on the other hand, didn't show any significant change in its wound healing capacity.

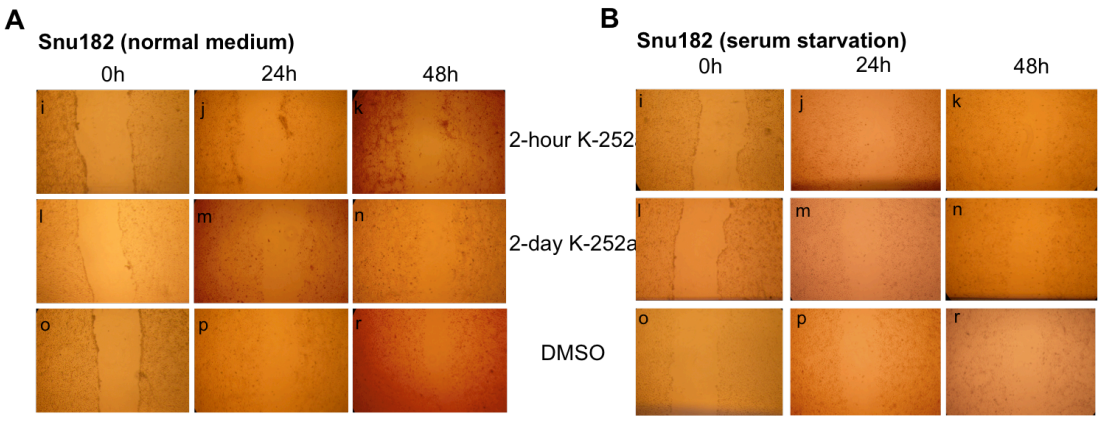

Figure 4. 9 Photographs of wound healing assay for Snu182 under (A) normal medium and (B) serum starved conditions and 2-hour inhibitor treatment (i, j, k), 2-day inhibitor treatment (l, m, n) and DMSO treatment as a control (o, p, r). (Magnification: 4x)

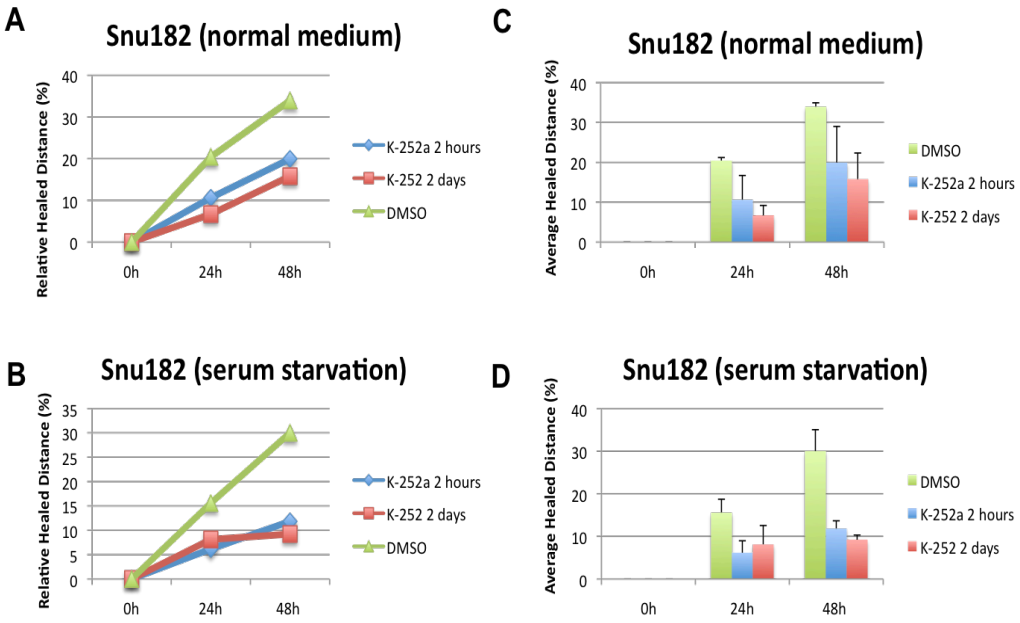

Figure 4. 10 Statistical analysis of Wound Healing Capacity of Snu182 in the presence and absence of inhibitor under normal (A, C) and serum starved conditions (B, D). Graphs A and B show the relative healed distance and C and D show the average healed distance of two experimental groups (p-value: NS between inhibitor treated and control groups).

Upon inhibitor treatment, Snu182 showed about 2-fold decrease in its healed distance in both normal medium (Figure 4.10A, C) and serum starved (Figure 4.10B, D) conditions. Also the two-hour and two-day inhibitor treatment showed similar effects. Snu398 also showed a decrease in its invasion ability. The decrease in the healing ability is also about 2-fold decrease in its healed distance in both normal medium (Figure 4.12A, C) and serum starved (Figure 4.12B, D) conditions.

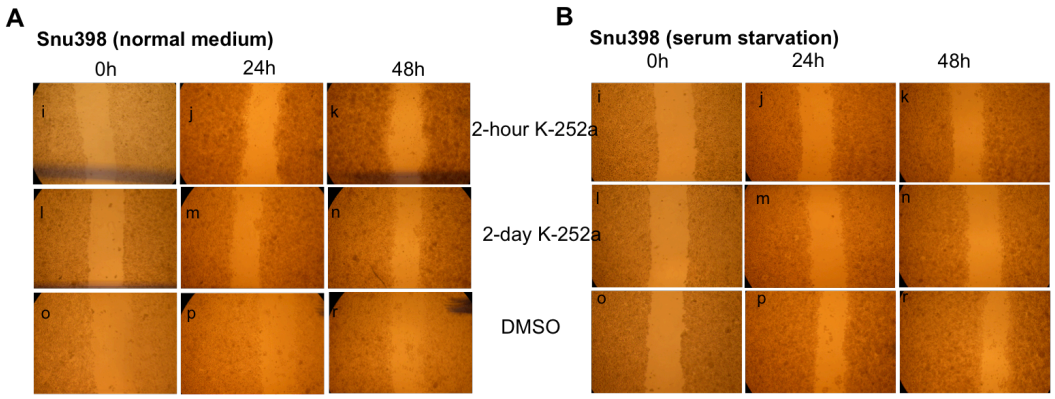

Figure 4. 11 Photographs of wound healing assay for Snu398 under (A) normal medium and (B) serum starved conditions and 2-hour inhibitor treatment (i, j, k), 2-day inhibitor treatment (l, m, n) and DMSO treatment as a control (o, p, r). (Magnification: 4x)

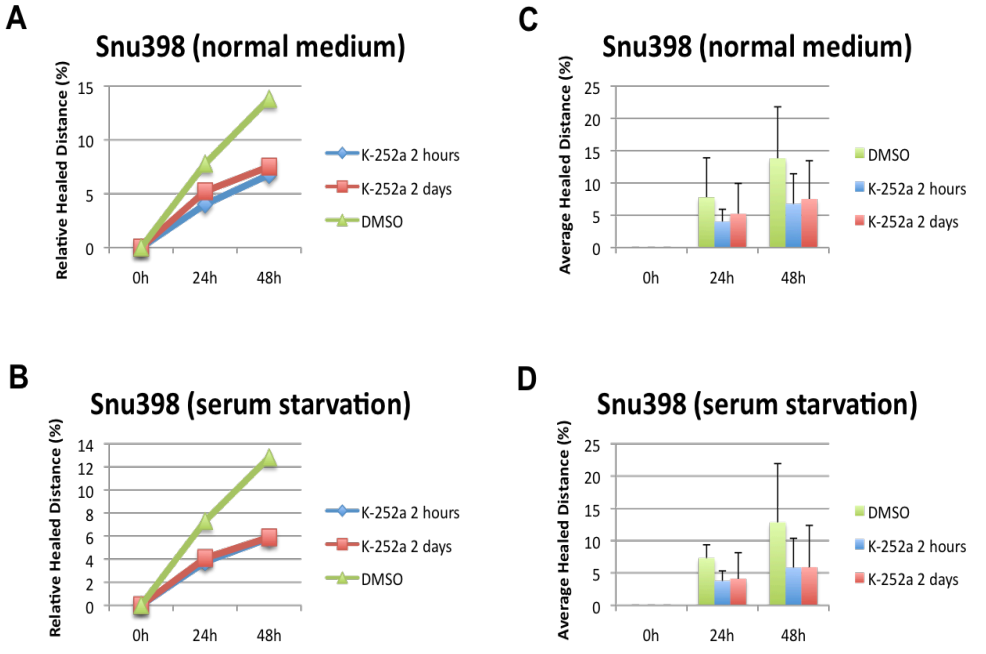

Figure 4. 12 Statistical analysis of Wound Healing Capacity of Snu398 in the presence and absence of inhibitor under normal (A, C) and serum starved conditions (B, D). Graphs A and B show the relative healed distance and C and D show the average healed distance of two experimental groups (p-value: NS between inhibitor treated and control groups).

On the other hand Huh7 didn't show any significant impairment in its invasion ability. Upon inhibitor treatment, the healed distance is similar to the distance in the absence of the inhibitor.

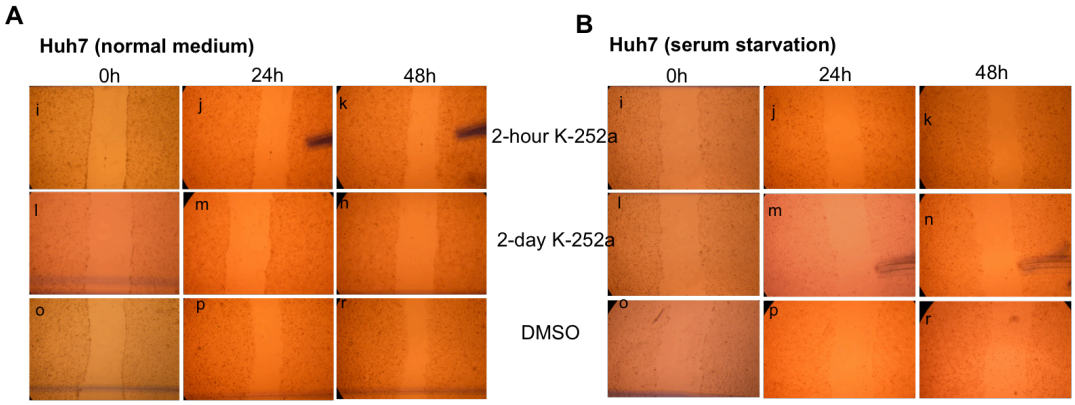

Figure 4. 13 Photographs of wound healing assay for Huh7 under (A) normal medium and (B) serum starved conditions and 2-hour inhibitor treatment (i, j, k), 2-day inhibitor treatment (l, m, n) and DMSO treatment as a control (o, p, r). (Magnification: 4x)

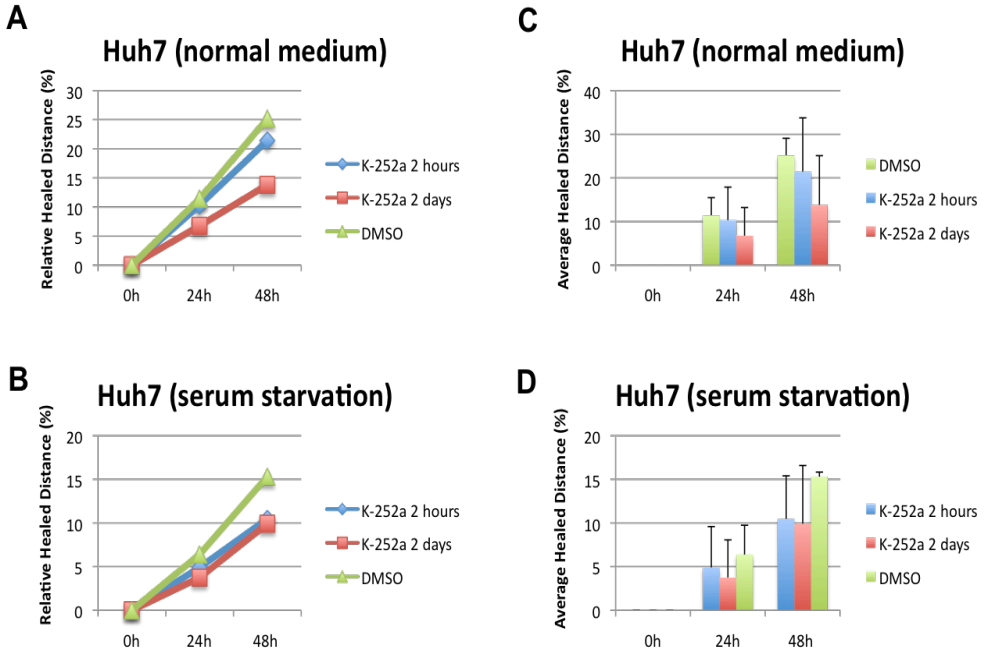

Figure 4. 14 Statistical analysis of Wound Healing Capacity of Huh7 in the presence and absence of inhibitor under normal (A, C) and serum starved conditions (B, D). Graphs A and B show the relative healed distance and C and D show the average healed distance of two experimental groups (p-value: NS between inhibitor treated and control groups).

4.3.4 Change in the Epithelial and Mesenchymal Lineage Markers After Inhibitor Treatment

After blocking the phosphorylation of FLT3 with its inhibitor K-252a, we observed decreased invasion ability of the cells Snu182, Snu398 and Hep40. We thought that this decrease in the invasion might also indicate a decrease in the migration of the cells and this could be due to the blocking of EMT. Therefore, we collected total RNA from Snu182, Snu398, Huh7 and Hep40, which were either treated with K-252a for 2 hours or DMSO. Expression levels of epithelial and mesenchymal markers were analyzed in the presence and absence of the

inhibitor with RT-PCR. Upon inhibitor treatment, no significant change is observed in the expression of any of these markers (Figure 4.15).

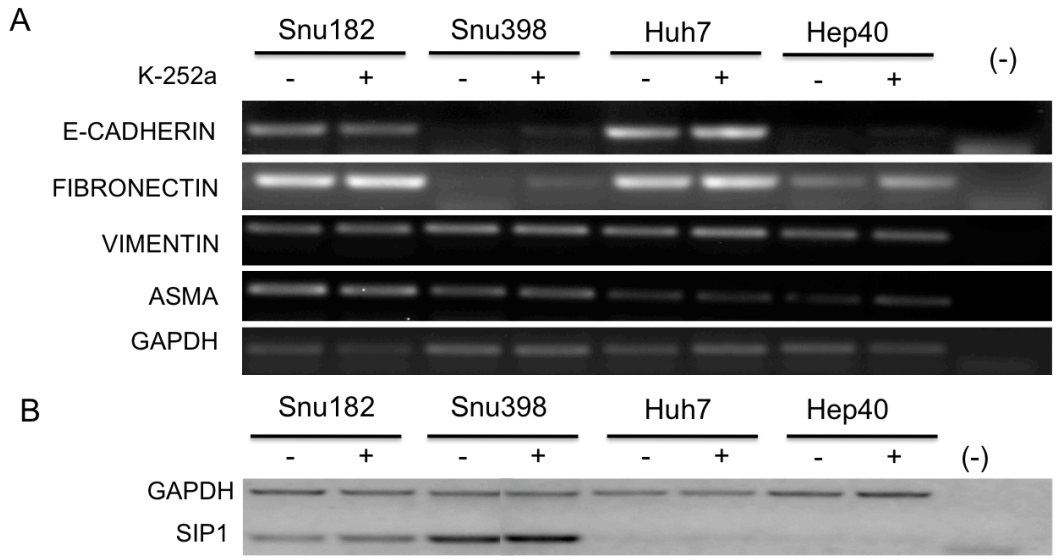

Figure 4. 15 RT-PCR analysis of Epithelial and Mesenchymal Lineage markers after 200nM K-252a treatment for two hours. (A) RT-PCR of E-cadherin, Fibronectin, Vimentin and ASMA. GAPDH is used as loading control. (B) Multiplex RT-PCR for Sip-1 and GAPDH. GAPDH is used as loading control.

4.3.5 *In vitro* Programmed Cell Death Analysis and Senescence Associated β-Gal Assay

4.3.5.1 In vitro Programmed Cell Death Analysis

In order to understand the mechanism behind the action of the inhibitor on FLT3, the induction of apoptosis and senescence in the presence and absence of the inhibitor is investigated. Upon inhibitor treatment for two hours, the fold changes in the number of apoptotic cells were calculated.

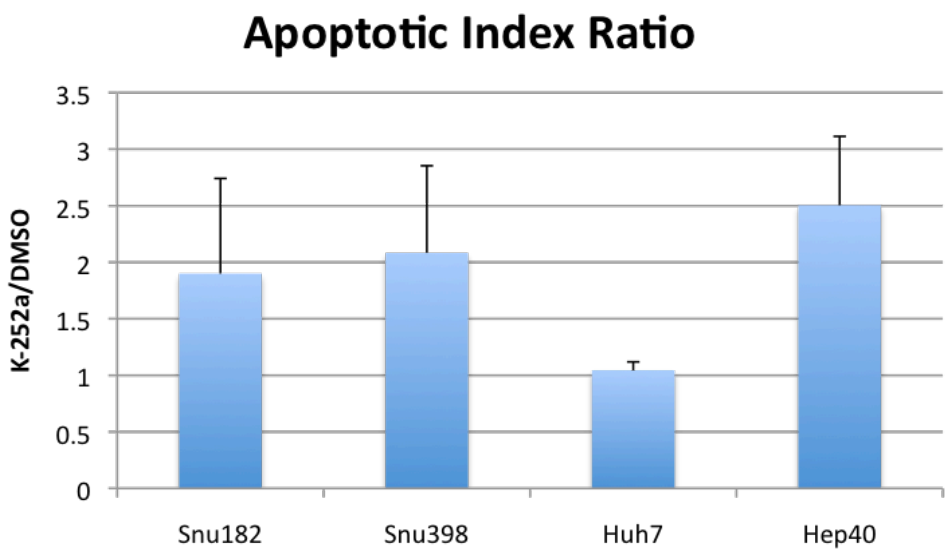

Figure 4. 16 The ratio of apoptotic indices of inhibitor treated cells and DMSO treated cells. Apoptotic cells were evaluated by TUNEL Assay (p-value: NS between inhibitor treated and control groups).

Inhibitor treatment caused about two-fold increase in apoptotic cells of Snu182 and Hep40, and more than 2-fold increase in Snu398 when compared against the number of apoptotic cells in the absence of the inhibitor. But its effect on Huh7 is very small (Figure 4.16).

4.3.5.2 Senescence-Associated β-Gal Assay

The role of FLT3 on cellular proliferation was established. Therefore to further asses the mechanisms which it exhibits its function, we checked whether cells enter to senescence upon inhibitor treatment. Cells that were seeded with 50% confluency were treated with K-252a for 2 hours prior to the assay. In Snu182 some senescent cells were observed but there was no induction of senescence after treatment with the inhibitor (Figure 4.17A,B). Snu398 didn't exhibit any senescent cells and this condition didn't vary with the presence of the inhibitor (Figure 4.17D, E). Huh7 contains more senescent cells compared to Snu182 and Snu398, but also no significant change in the number of senescent

cell was observed upon 2-hour inhibitor treatment (Figure 4.17G, H). Finally the same case was true for Hep40. Upon inhibitor treatment, no induction in the senescence was observed (Figure 4.17J, K). As negative control, SABG solution without X-gal was used and no staining was observed (Figure 4.17C, F, I, L).

So collectively, FLT3 inhibitor didn't show any induction of senescence in Snu182, Snu398, Huh7 and Hep40.

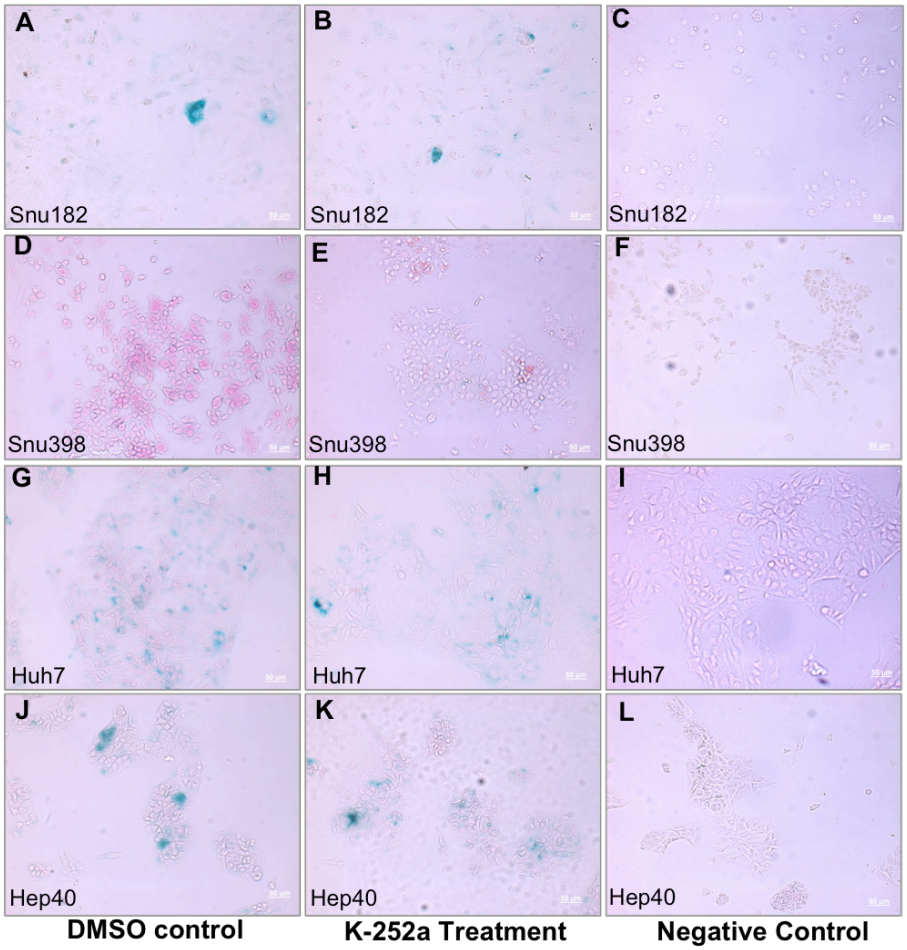

Figure 4. 17 SABG staining of Snu182, Snu398, Huh7 and Hep40 in the absence (A, D, G, J) and presence (B, E, H, K) of the inhibitor. As negative control, SABG solution without X-gal is used (C, F, I, L).

4.4 *In vivo* Tumorigenesis

Our in vitro data have strongly suggested a role for FLT3 in invasiveness of the HCC cell lines that we tested. In this part of my thesis, I aimed to test its role in tumorigenesis at the in vivo conditions by using xenograft models in nude mice. To investigate the tumor forming ability of Snu182, Snu398, Huh7 and Hep40, cells were treated with 200nM K-252a for two hours prior to injection. Control cells were treated with equal volume of DMSO for two hours. 6 million cells/250μL per animal was injected subcutaneously to male nude mouse. Inhibitor-treated cells and control cells were injected subcutaneously into the same animal (right and left side of the dorsal region of the mice, respectively). Our results showed that Snu182 injected animals didn't form any tumors for a time course of 3 months. Snu398 injected animals showed fastest tumor formation. Inhibitor treated Snu398 cells didn't showed any tumor, where the control cells formed tumors two weeks after injection (Figure 4.18 and Figure 4.21). Figure 4.18 shows the growth of the tumors after injection. Figure 4.21 on the other hand shows the average sizes of the tumors of all the animals that formed tumors after injection. The difference between the tumor forming abilities of inhibitor treated and control cells of Snu182 are significant with a p-value of 0.045 (Figure 4.21).

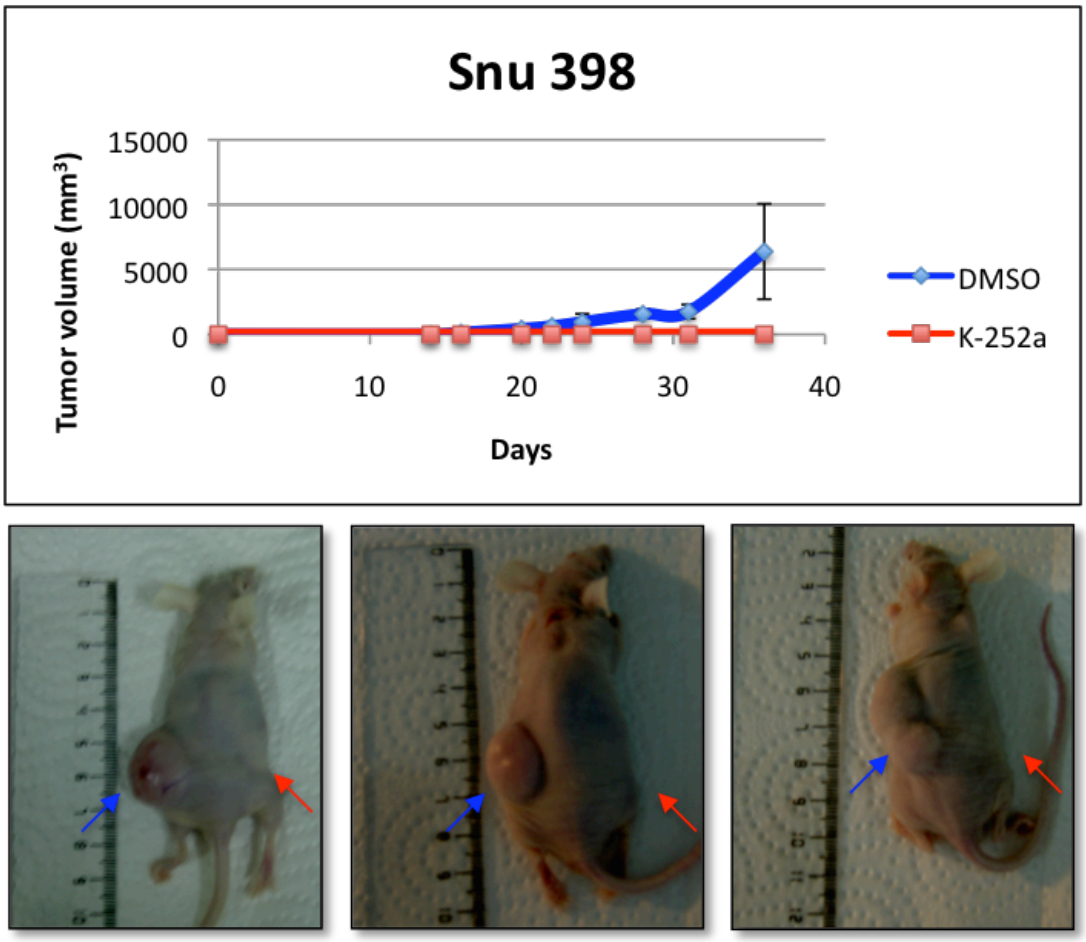

Figure 4. 18 Xenograft Tumors of Snu398. In the graph, growth of the tumor volume can be observed. In the photographs, tumors of three different nude mice are seen. (Blue arrows: DMSO treated cells' injection site, Red arrows: K-252a treated cells' injection site)

Similarly, Hep40 cells also showed significant difference in tumor formation in the absence and the presence of the inhibitor. Tumors at sites where control cells of Hep40 were injected started to appear 2 weeks after injection (Figure 4.19). Hep40 cells treated with inhibitor also formed tumors but the sizes of the tumors are significantly (p-value: 0.009) smaller than the tumors formed by the control cells (Figure 4.21).

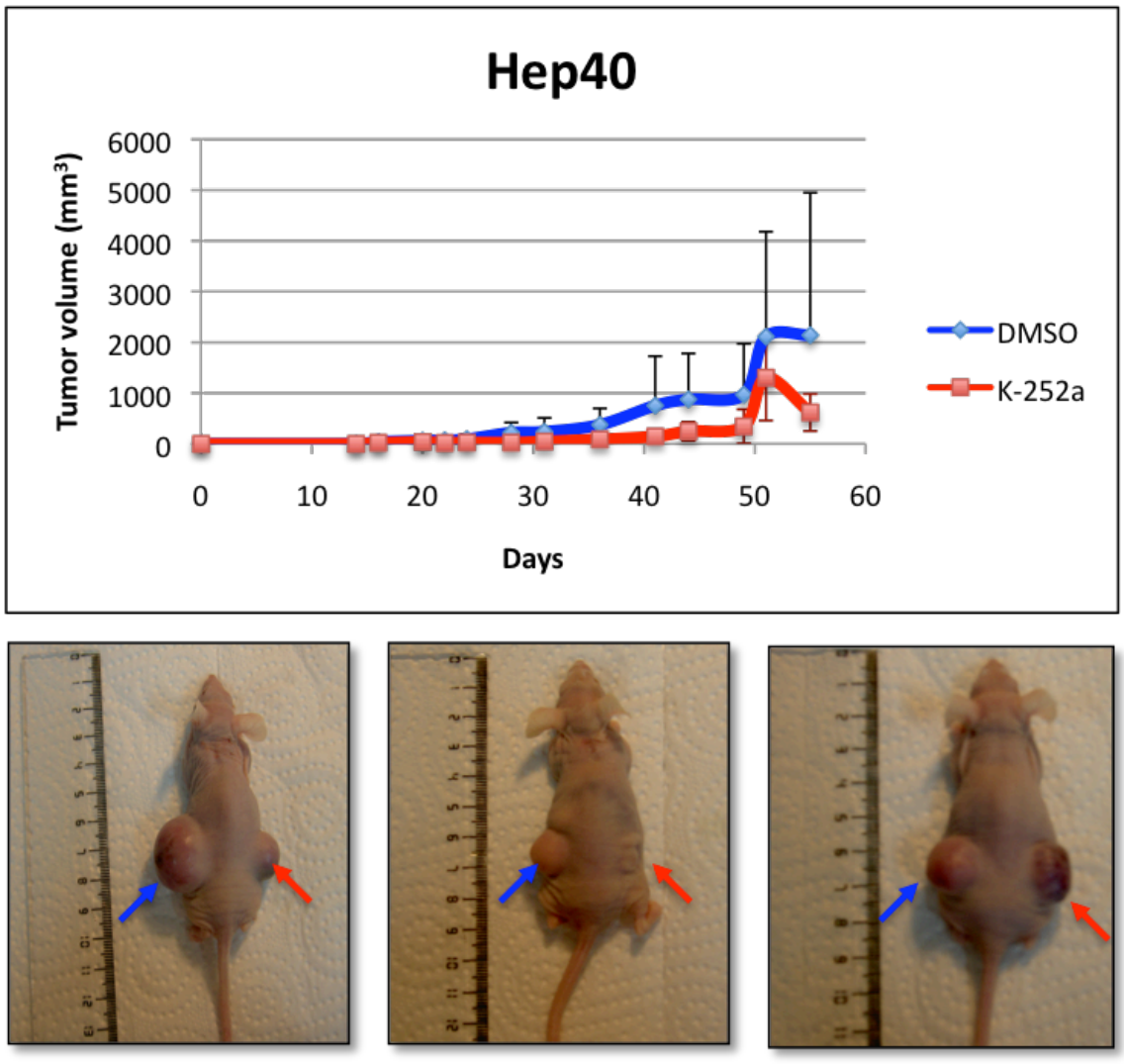

Figure 4. 19 Xenograft Tumors of Hep40. In the graph, growth of the tumor volume can be observed. In the photographs, tumors of three different nude mice are seen. (Blue arrows: DMSO treated cells' injection site, Red arrows: K-252a treated cells' injection site)

On the other hand, Huh7 injected animals didn't give any significant results (Figure 4.21). Tumors appeared later than Snu398 and Hep40, on day 35 after injection and there wasn't any significant difference between the sizes of tumors formed by inhibitor treated cells or control cells. On day 55 after the injection, one of the animals with Huh7 tumors had to be euthanized due to the tumors necrosis. Figure 4.20 shows the growth of the tumors until day 55. But the

recording of tumor sizes continued form the remaining animals and the remaining animals showed larger tumors in sites where inhibitor treated cells were injected (data not shown).

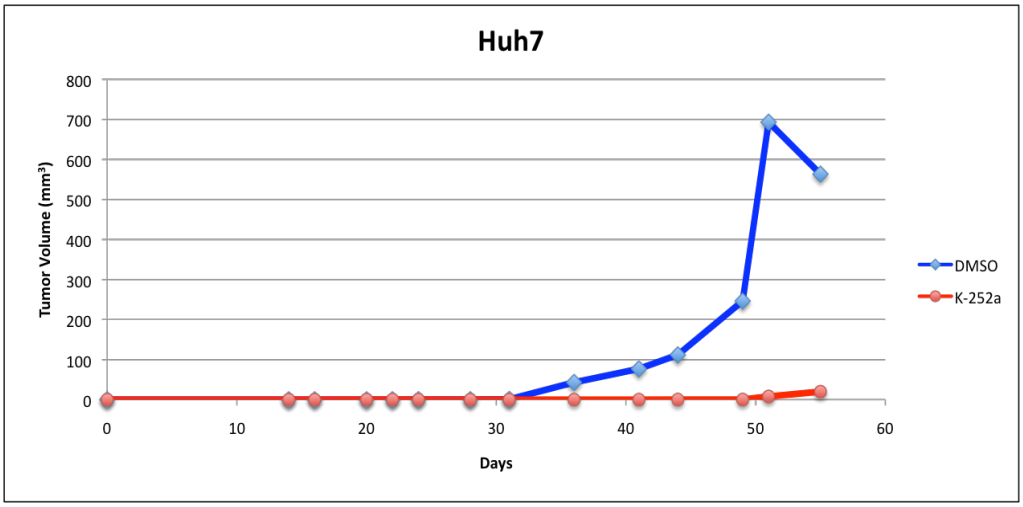

Figure 4. 20 Xenograft Tumors of Huh7. In the graph, growth of the tumor volume can be observed. The average tumor volume of 4 animals until day 55 was shown.

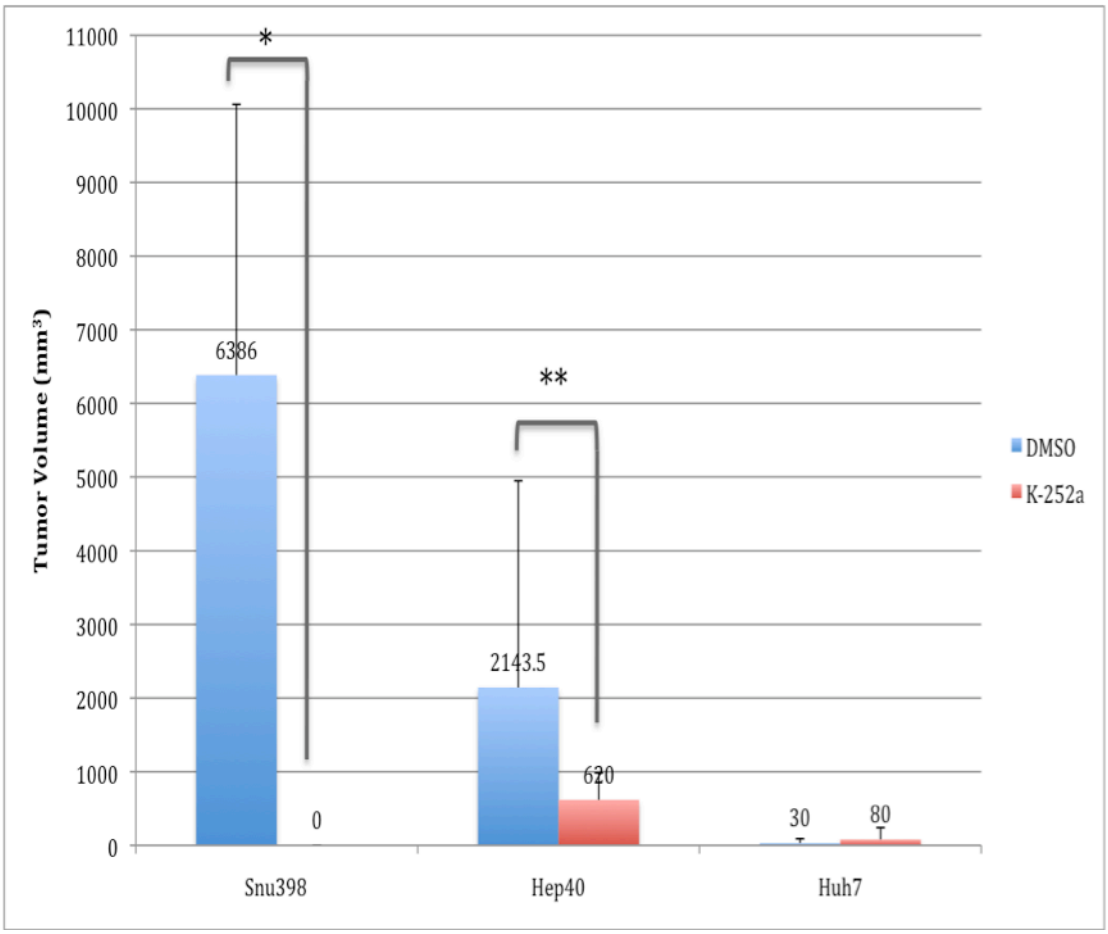

Figure 4. 21 Average tumor volumes of xenografts injected with Snu398, Hep40 and Huh7 cells in the presence or absence of inhibitor. (*: p-value=0.045, **: p-value=0.009)

These results indicate that; inhibitor treatment of Snu398 and Hep40 showed significant impairment in the tumor forming ability of these cell lines, but it has no significant effect on Huh7. These results are also consistent with the *in vitro* invasion capacities of the cell lines.

Collectively our results indicate that FLT3 plays an important role in hepatocellular carcinogenesis.

5. Discussion

5.1 Discussion

Liver is the one of the vital organs in the body and has been an interest for research even in ancient times. Its important biological functions, such as detoxification and regenerative capacity differentiate liver from many other organs in the body. Therefore it is not surprising that hepatocellular carcinoma is one of the most lethal cancers all over the world. In addition, consistent biomarkers to characterize HCCs and different stage liver diseases ranging from regenerating liver, fibrosis and cirrhosis are missing. Lack of biomarker is one of the main obstacles behind good diagnostic and prognostic tools. The only cure of end-stage liver diseases is liver transplantation, however the need for organ for transplantation is by far less than the availability (http://organdonor.gov). As of July 2010, there are 108,091 patients who are waiting for the transplant. The number of the donors for the period of January-March 2010 was only 3,440. Therefore the need for biomarker for early diagnosis is more than ever. Such markers can also be good candidates against targeted therapeutical approaches.

Molecular characterization of HCCs is very important, since its characterization is the indicator of the prognosis of the disease. There are recent microarray based comparative genomic researches aimed to identify a molecular structure for HCCs of different stages (Colak et al, 2010). Today the major characterization of HCC is based on the Alfa-feta protein expression levels and the stemness of the tumor cells, which gives the definitions of WD and PD (Qin and Tang, 2002). However, this characterization is too wide to be used as a marker for diagnostic and therapeutic purposes. We adopted a different rationale to identify a candidate marker in hepatocellular carcinogenesis. We focused on FLT3 in order to differentiate between HCCs for the following reasons:

i) Involvement of tyrosine kinases in development of malignancies (Lemmon and Schlessinger, 2010)

ii) By our group FLT3 has been shown to play a role during liver regeneration (Aydin et al, 2007)

iii) Close relation of hematopoietic stem cells during liver development and hematopoiesis (Kinoshita et al, 1999) indicates that FLT3 might also function during liver development.

iv) Role of FLT3 in AML (Thiede et al, 2002 and Nakao et al, 1996)

Therefore, first we analyzed the expression level of FLT3 in 14 HCC cell lines. Our data showed that FLT3 was expressed in Snu182, Snu398 (PD) and Hep40 (WD) on mRNA level and in Hep3B, Hep40 (WD) and Focus, SK-Hep1, Snu182, Snu387 and Snu398 (PD) on protein level (Figure 4.1 and Figure 4.2). These results suggest that there is no correlation between the expression of FLT3 and the differentiation status of the HCC cell lines. Thus, after checking the expression of FLT3, we wanted to analyze these 14 HCC cell lines for expression of a range of stem cell markers and epithelial and mesenchymal lineage markers.

One of the markers that we analyzed was CD133, which is a hematopoietic progenitor marker. More importantly it is highly associated with cancer stem cells, where the subpopulations of $CD133^+$ cells are able to form tumors in xenograft models. Although it is related to stemness properties, it was interesting to observe its expression in WD HCC cell lines (HepG2, Hep3B, Hep40, Huh7 and PLC). This could be an indication for the presence of cancer stem cells in these well-differentiated HCC cell lines. In fact the presence of a $CD133^+$ subpopulation of cells was shown to be tumorigenic in Huh7 cell line (Yin et al, 2007). Besides the WD HCCs, PD HCC cell lines (Mahlavu, Focus, Snu182 and Snu449) showed CD133 expression. Since the PD HCC cell lines

resemble stem cells, it is reasonable to observe the expression of CD133, but whether this expression comes form a subpopulation of cells that could be inferred as cancer stem cells or the expression is universal should be investigated (Figure 4.3).

The second marker that we analyzed is CD90, which is a mesenchymal stem cell marker. We observed its expression mainly in PD HCC cell lines (Focus, SK-Hep-1, Snu387 and Snu398). The expression of CD90 could also be used to differentiate WD and PD HCCs, in order to predict the prognosis of the disease (Figure 4.3).

Thirdly, we performed RT-PCR for LGR5. LGR5 is an orphan G-protein coupled receptor, which was initially identified as a marker of stem cells in +4 position of the intestinal crypts (Barker et al, 2007). This adult stem cell marker was then found to be expressed in many other organ's adult stem cells ranging from colon to hair follicle and in some cancer types such as colorectal cancer (Barker et al 2008). These evidences also suggests that LGR5 can also be used the characterize HCC cell lines, both because of its indication of stem cell properties (Figure 4.3).

Since there is a close correlation between liver development and hematopoiesis, where fetal liver is the site for hematopoiesis (Kinoshita et al, 1999), we analyzed the expression levels of some hematopoietic markers. All the cell lines tested were negative for CD45 and only Snu182 showed expression of CD34. This suggests that Snu182, which is a poor differentiated HCC, resembles the early progenitors of hepatic cells and hematopoietic cells (Figure 4.3).

Also this expression analysis revealed an interesting relation between Snu182 and Snu398. Although these two cells lines are FLT3 positive both on mRNA and protein level, when the expressions of other markers are analyzed, they have showed different characteristics. Snu182 is positive for CD133, LGR5

and CD34 where Snu398 is positive for CD90 and negative for the rest of the markers. This could indicate that FLT3 might be a marker of different types of HCCs with different molecular characteristics, which widens its diagnostic and therapeutic applications.

For further characterization, we analyzed epithelial and mesenchymal lineage markers. EMT is a very important process during development and cancer. By analyzing the expression of some epithelial and mesenchymal lineage markers, it is aimed understand the different stages of hepatocellular carcinogenesis and the consequence of epithelial or mesenchymal originated cells to the outcome of the cancer. The mesenchymal lineage markers vimentin and α-SMA didn't reveal any expression differences between 14 HCC cell lines. On the other hand fibronectin, which is also a mesenchymal lineage marker, was expressed in all of the cell lines, but its expression varies. E-cadherin's expression is restricted to WD HCC and Snu182. Snu182 and Snu398 again showed different characteristics, where Snu182 is E-cadherin positive and highly expressed fibronectin and Snu398 is E-cadherin negative and slightly expressed fibronectin (Figure 4.4). Also the co-expression of both epithelial and mesenchymal markers indicates that these cell lines contain heterogeneous cell populations. This situation resembles the *in vivo,* where the tumors have heterogeneity (An et al, 2001).

After the characterization of HCC cell lines, we also checked the expression pattern of FLT3 in normal (Figure 4.5) and cirrhotic (Figure 4.6) liver human tissue sections. In normal liver, FLT3 is only observed in cells near the ductal structure, which might be the progenitor cells of the liver (Sell and Leffer, 2008). But on the other hand, we observed an extensive patchy appearance of cytoplasmic FLT3 expression by the hepatocytes in cirrhotic liver. But to further conclude that FLT3 expression varies between regenerating, fibrotic, cirrhotic livers and HCC, a larger array of tissue sections are needed.

The subcellular localization of FLT3 infers some functional differences. Previous results had shown that upon PH, in a rat liver regeneration model, membrane bound FLT3 becomes cytoplasmic (Aydin et al, 2007). Interestingly our immunofluoroscent staining has shown that FLT3 has a nuclear staining in Snu182, Snu398 and Hep40 (Figure 4.8). FLT3-ITD mutants also showed an abnormal localization, in perinuclear regions and in different compartments of secretory pathway (Koch et al, 2008). These results indicate that the localization of the protein might cause differences in its functionality.

After the characterization of the cell lines and identifying the localization of FLT3 in liver sections and cell lines, we decided to perform functional analysis of FLT3, which is necessary to link the expression of the protein with hepatocellular carcinogenesis. For this purpose, we used FLT3 inhibitor K-252a, which blocks the signal transduction of the protein via blocking its phosphorylation. First of all, whether the subcellular localization of the protein changes after the inhibitor treatment is checked. Interestingly, blocking the function of the FLT3 with K-252a caused the protein to more accumulate in the nucleus and endoplasmic reticulum, as opposed to the membrane bound localization expected (Figure 4.8). This suggests that FLT3 has an auto-regulatory role in the sorting of the protein. Also these results support the conclusion where the localization of the proteins is important for its function.

To further analyze the involvement of FLT3 in HCC progression, we used an *in vitro* invasion assay, wound healing assay. We performed the assay with normal medium conditions (10% FBS) and under low serum conditions, which we referred as serum starvation (2% FBS) throughout the thesis. By serum starving the cells, we stop their proliferation and therefore aim to see only the invasion of the cells. After the wounds were made, cells were treated with the FLT3 inhibitor for two hours or for two days. Our results revealed that Snu182 and Snu398 showed an approximate of two fold decrease in their invasion capacity under the

influence of the inhibitor for both 2 hours and 2 days (Figure 4.10 and Figure 4.12). Also the results are consistent for both serum starvation and normal medium, which indicates that the effect is not due to stalled proliferation but due to the invasion of the cells. On the other hand, we couldn't observe any change in the invasion capacity of Huh7 in the presence and in the absence of the inhibitor (Figure 4.14). This result is expected, since Huh7 didn't express FLT3. This negative control also indicated that the effect of the inhibitor is more or less specific to FLT3 phosphorylation.

This invasion capacity might also be an indicator for migration capacity of the cells. After inhibitor treatment, any change that occurs in the expression of epithelial and mesenchymal markers could indicate the process of EMT/MET, which could explain the role of FLT3 in the metastasis of the cells. Recently, EMT has been shown to play an important role in hepatocellular carcinogenesis (Choi and Diehl, 2009). Upon inhibitor treatment, we did not observe any change in the expression levels of these markers suggesting that the role of FLT3 on tumorigenesis is not through inducing EMT (Figure 4.15). New studies such as *in vitro* migration assays are warranted to clarify this issue.

FLT3 has proliferative and anti-apoptotic roles. Its signal transduction involves the inhibition of apoptotic genes and activation of MAPK and PI3K pathways (Stirewalt and Radich, 2003). To see whether there will be any change between the number of apoptotic cells in the absence and the presence of the inhibitor, we performed TUNEL assay. Upon inhibitor treatment we observed about 2-fold increase in the number of apoptotic cells in Snu182, Snu398 and Hep40. As in the case of wound healing assay results, Huh7 didn't show any change in the number of apoptotic cells (Figure 4.16). These results indicate that activating anti-apoptotic mechanisms is could be one of the mechanisms FLT3 contributes to tumorigenesis *in vivo*. This case was also shown for the case of AML, where 25-45% of the AML patients have a constitutively activating

mutation of FLT3 (Stirewalt and Radich, 2007). A study in AML, treatment with a different FLT3 inhibitor (PKC412) showed increased apoptosis. Also the same study showed that using a FLT3 inhibitor, in combination with drug that induces apoptosis (C-28 methyl ester of the oleane triterpenoid) increases the apoptosis (Ahmad et al, 2010). This suggests that combinations of therapies that include FLT3 inhibitors and other chemotherapeutic agents can also be used in different types of HCCs.

Since FLT3 signaling also activates pathways related to proliferation, we checked whether absence of this signaling induces senescence. We performed senescence-associated β-Gal assay after 2-hour inhibitor treatment. We used DMSO for control treatments. Our results show no difference in any of the cell lines (Snu182, Snu398, Huh7 and Hep40) between the inhibitor treated cells and control cells (Figure 4.17). This indicates that the tumorigenesis of FLT3 is not supported by inactivation of senescence.

Our *in vitro* data suggest the involvement of FLT3 in the invasiveness of the HCC cell lines, but EMT does not occur during this process. To see whether it has a role in tumorigenesis, we used xenograft models in nude mice. Snu398 formed tumors only with the control cells but no tumors are formed at the site of injection of inhibitor treated cells (p-value: 0.045). Hep40 cells formed significantly smaller tumors in inhibitor treated samples (p-value: 0.009)(Figure 4.21). These data provide strong evidence to the involvement of FLT3 in hepatocellular carcinoma formation *in vivo*. Subcutenous injection of Huh7 cells, on the other hand, formed tumor with inhibitor-treated and control-treated groups, but there was no significant difference in terms of tumor sizes. Interestingly, Snu182 cells didn't form any tumors. The reason of the discrepancy in terms of the tumor formation between Snu398 and Snu182 might be due to the differences of the expressions of the markers that we tested in this thesis. Besides the expression of FLT3, all the markers showed different expression patterns in

Snu182 and Snu398 cell lines (Table 5.1). As seen from this table, Snu182 was positive for CD133. This data might be seen as controversial since CD133 is a cancer stem cell marker, however it is in parallel with a recent study which showed that expression of cancer stem cells markers cannot be considered as the only prognostic parameters in HCCs (Salnikov et al, 2009).

Figure 5.1 briefly summarizes the relations between FLT3 throughout the progression of HCC from normal liver. In normal liver, FLT3 is expressed only in progenitor cells. Upon injury, it is changes its localization and participates in the regeneration process (Aydin et al, 2007). We have shown that FLT3 is extensively expressed by the hepatocytes in cirrhotic liver, with a patchy appearance in the tissue.

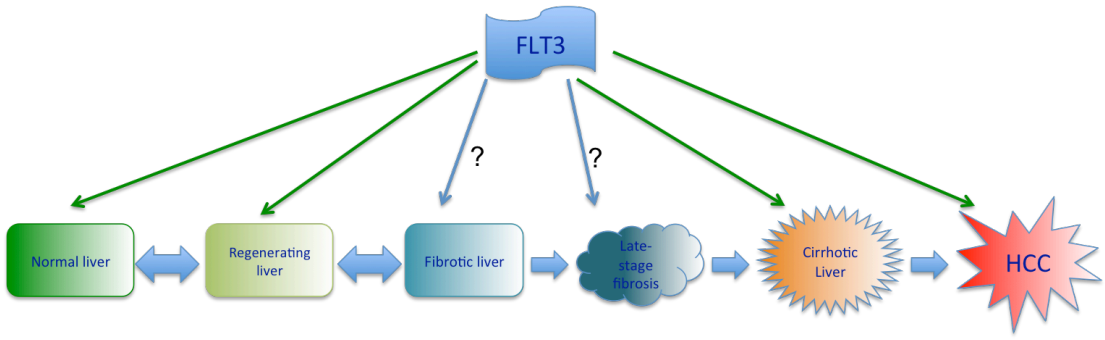

Figure 5. 1 FLT3's involvement during different stages leading to HCC. The question marks in the figure indicate the areas where we need further investigation. Green arrows belong to the relations mentioned and revealed in this thesis.

Our findings of *in vitro* and *in vivo* experiments are summarized in Table 5.1. Collectively, our results revealed that FLT3 contributes to hepatocellular carcinogenesis as shown by both *in vitro* and *in vivo* assays. Also, its expression in HCC cell lines together with different molecular subtypes (with different marker expression) indicates that it can be a diagnostic tool for HCCs from different stages. As in the case of AMLs it can also be a good therapeutic candidate for the treatment of HCCs, since blocking its activity showed severe impairment in the tumor forming ability.

Table 5. 1 Findings of *in vitro* and *in vivo* experiments

	FLT3 mRNA level	FLT3 Protein Level	LGR5 mRNA level	CD133 mRNA level	CD90 mRNA level	CD45 mRNA level	CD34 mRNA level	E-cad mRNA level	Fibronectin mRNA level	ASMA mRNA level	Invasiveness		Tumorigenesis	
											DMSO	K-252a	DMSO	K-252a
HepG2	-	-	***	*	-	-	-	-	**	****	N/A	N/A	N/A	N/A
Hep3B	-	*	****	*****	-	-	-	***	*	**	N/A	N/A	N/A	N/A
Hep40	*	*	-	*	*	-	-	-	*	**	N/A	N/A	***	*
Huh7	-	-	**	****	-	-	-	*	*	*	**	**	**	**
PLC	-	-	*	***	-	-	-	*	*	*	N/A	N/A	N/A	N/A
Mahlavu	-	-	-	**	*	-	-	-	*	****	N/A	N/A	N/A	N/A
Focus	-	-	-	*	**	-	-	-	*	***	N/A	N/A	N/A	N/A
SK-Hep-1	-	*	-	-	***	-	-	-	****	****	N/A	N/A	N/A	N/A
Snu182	***	*	***	**	-	-	**	**	****	****	**	*	-	-
Snu387	-	*	-	-	****	-	-	-	**	***	N/A	N/A	N/A	N/A
Snu398	**	***	-	-	***	-	-	-	*	**	**	*	***	-
Snu423	-	-	-	-	-	-	-	-	**	****	N/A	N/A	N/A	N/A
Snu449	-	-	-	*	-	-	-	-	*	***	N/A	N/A	N/A	N/A
Snu475	-	-	*	-	-	-	-	-	***	****	N/A	N/A	N/A	N/A

5.2 Future Perspectives

Our data in this thesis provide essential information regarding the role of FLT3 in hepatocellular carcinogenesis. In order to have an entire picture of molecular mechanisms of HCC development and FLT3, it is imperative to extend our studies in the following direction as depicted in figure 5.1:

- FLT3 in fibrotic livers should be further analyzed with tissue samples from varying stages of fibrotic and cirrhotic livers.
- Although significant results were obtained with FLT3 inhibitor, siRNA knockdown studies should be performed against FLT3. Migration and invasion assays as well as *in vivo* xenograft experiments should be performed after knocking down the FLT3 with lentiviral systems in order to better understand the role of this protein during hepatocarcinogenesis.
- FLT3 mutations were found in many AML patients, to check whether FLT3 is also mutated in HCCs, mutational analysis should be performed for FLT3 for the most common constitutively activating mutations.
- Finally, crosstalk between FLT3 signaling and immune response should also be explored in order to shed light into the mechanism of hepatocarcinogenesis. Role of TLRs during this process would provide important information to design appropriate therapeutic approaches to tackle HCC.

6. References

A history of The Liver, Spleen and Gallbladder, Stanford University [online], http://www.stanford.edu/class/history13/earlysciencelab/body/liverpages/livergallbladderspleen.html (2010).

Ahmad R, Liu S, Weisberg E, Nelson E, Galinsky I, Meyer C, Kufe D, Kharbanda S, Stone R, (2010). **Combining the FLT3 Inhibitor PKC412 and the Triterpenoid CDDO-Me Synergistically Induces Apoptosis in Acute Myeloid Leukemia with the Internal Tandem Duplication Mutation**, *Mol Cancer Res*. Jun 22 [Epub ahead of print].

Al-Hajj M, Wicha MS, Benito-Hernandez A, Morrison SJ, Clarke MF, (2003). **Prospective identification of tumorigenic breast cancer cells**, *Proc Natl Acad Sci U S A*. 100(7):3983-8.

American Cancer Society, Cancer Facts and FIGS 2010, American Cancer Society [online], http://www.cancer.org/downloads/STT/Cancer_Facts_and_Figures_2010.pdf (2010).

An FQ, Matsuda M, Fujii H, Tang RF, Amemiya H, Dai YM, Matsumoto Y, (2001). **Tumor heterogeneity in small hepatocellular carcinoma: analysis of tumor cell proliferation, expression and mutation of p53 AND beta-catenin**, *Int J Cancer*. 93(4):468-74.

Aydin IT, Tokcaer Z, Dalgic A, Konu O, Akcali KC, (2007). **Cloning and expression profile of FLT3 gene during progenitor cell-dependent liver regeneration**, *J Gastroenterol Hepatol*. (12):2181-8.

Barker N, van Es JH, Jaks V, Kasper M, Snippert H, Toftgård R, Clevers H, (2008). **Very long-term self-renewal of small intestine, colon, and hair**

follicles from cycling Lgr5+ve stem cells, *Cold Spring Harb Symp Quant Biol*. 73:351-6.

Barker N, van Es JH, Kuipers J, Kujala P, van den Born M, Cozijnsen M, Haegebarth A, Korving J, Begthel H, Peters PJ, Clevers H, (2007). **Identification of stem cells in small intestine and colon by marker gene Lgr5**, *Nature*. 449(7165):1003-7.

Bataller R, Brenner DA, (2005). **Liver fibrosis,** *J Clin Invest*. 115(2):209-18.

Blouin A, Bolender RP, Weibel ER, (1977). **Distribution of organelles and membranes between hepatocytes and nonhepatocytes in the rat liver parenchyma. A stereological study**, *J Cell Biol*. 72(2):441-55.

Brasel K, Escobar S, Anderberg R, de Vries P, Gruss HJ, Lyman SD, (1995). **Expression of the flt3 receptor and its ligand on hematopoietic cells,** *Leukemia*. 9(7):1212-8.

Brazel CY, Ducceschi MH, Pytowski B, Levison SW, (2001). **The FLT3 tyrosine kinase receptor inhibits neural stem/progenitor cell proliferation and collaborates with NGF to promote neuronal survival,** *Mol Cell Neurosci*. 18(4):381-93.

Bort R, Signore M, Tremblay K, Martinez Barbera JP, Zaret KS, (2006). **Hex homeobox gene controls the transition of the endoderm to a pseudostratified, cell emergent epithelium for liver bud development***, Dev Biol*. 290(1):44-56.

Chen Z, Qi LZ, Zeng R, Li HY, Dai LJ, (2010). **Stem cells and hepatic cirrhosis**, *Panminerva Med*. 52(2):149-65.

Chiba T, Kita K, Zheng YW, Yokosuka O, Saisho H, Iwama A, Nakauchi H, Taniguchi H, (2006). **Side population purified from hepatocellular carcinoma cells harbors cancer stem cell-like properties**, *Hepatology*. 44(1):240-51.

Colak D, Chishti MA, Al-Bakheet AB, Al-Qahtani A, Shoukri MM, Goyns MH, Ozand PT, Quackenbush J, Park BH, Kaya N, (2010). **Integrative and comparative genomics analysis of early hepatocellular carcinoma differentiated from liver regeneration in young and old**, *Mol Cancer*. 9:146.

Cools J, Mentens N, Furet P, Fabbro D, Clark JJ, Griffin JD, Marynen P, Gilliland DG, (2004). **Prediction of resistance to small molecule FLT3 inhibitors: implications for molecularly targeted therapy of acute leukemia**, *Cancer Res*. 64(18):6385-9.

Choi SS, Diehl AM, (2009). **Epithelial-to-mesenchymal transitions in the liver**, *Hepatology*. 50(6):2007-13.

Dabeva MD, Shafritz DA, (1993). **Activation, proliferation, and differentiation of progenitor cells into hepatocytes in the D-galactosamine model of liver regeneration,** *Am J Pathol*. 143(6):1606-20.

Drexler HG, Quentmeier H, (2004). **FLT3: receptor and ligand**, *Growth Factors*. 22(2):71-3.

Enzan H, Hara H, Yamashita Y, Ohkita T, Yamane T, (1983). **Fine structure of hepatic sinusoids and their development in human embryos and fetuses**, *Acta Pathol Jpn*. 33(3):447-66.

Evans MJ, Kaufman MH, (1981). **Establishment in culture of pluripotential cells from mouse embryos,** *Nature*. 292(5819):154-6.

Farazi PA, DePinho RA, (2006). **Hepatocellular carcinoma pathogenesis: from genes to environment**, *Nat Rev Cancer*. 6(9):674-87.

Fausto N, Campbell JS, (2003). **The role of hepatocytes and oval cells in liver regeneration and repopulation,** *Mech Dev*. 120(1):117-30.

Friedman SL, (2008). **Hepatic stellate cells: protean, multifunctional, and enigmatic cells of the liver,** *Physiol Rev*. 88(1):125-72.

Garcia-Tsao G, Friedman S, Iredale J, Pinzani M**,** (2010). **Now there are many (stages) where before there was one: In search of a pathophysiological classification of cirrhosis,** *Hepatology*. 51(4):1445-9.

Gressner AM, Weiskirchen R, (2006). **Modern pathogenetic concepts of liver fibrosis suggest stellate cells and TGF-beta as major players and therapeutic targets**, *J Cell Mol Med*. 10(1):76-99.

Gupta PB, Chaffer CL, Weinberg RA, (2009). **Cancer stem cells: mirage or reality?,** *Nat Med*. 15(9):1010-2.

Hannum C, Culpepper J, Campbell D, McClanahan T, Zurawski S, Bazan JF, Kastelein R, Hudak S, Wagner J, Mattson J, et al., (1994). **Ligand for FLT3/FLK2 receptor tyrosine kinase regulates growth of haematopoietic stem cells and is encoded by variant RNAs**, *Nature*. 368(6472):643-8.

Hernández-Muñoz R, Díaz-Muñoz M, Suárez J, Chagoya de Sánchez V, (1990). **Adenosine partially prevents cirrhosis induced by carbon tetrachloride in rats,** *Hepatology*. 12(2):242-8.

Kalluri R, Weinberg RA, (2009). **The basics of epithelial-mesenchymal transition**, *J Clin Invest*. 119(6):1420-8.

Kenins L, Gill JW, Holländer GA, Wodnar-Filipowicz A, (2010). **Flt3 ligand-receptor interaction is important for maintenance of early thymic progenitor numbers in steady-state thymopoiesis**, *Eur J Immunol*. 40(1):81-90.

Kinoshita T, Sekiguchi T, Xu MJ, Ito Y, Kamiya A, Tsuji K, Nakahata T, Miyajima A, (1999). **Hepatic differentiation induced by oncostatin M attenuates fetal liver hematopoiesis,** *Proc Natl Acad Sci U S A*. 96(13):7265-70.

Koch S, Jacobi A, Ryser M, Ehninger G, Thiede C, (2008). **Abnormal localization and accumulation of FLT3-ITD, a mutant receptor tyrosine kinase involved in leukemogenesis,** *Cells Tissues Organs*. 188(1-2):225-35.

Lemmon MA, Schlessinger J, (2010). **Cell signaling by receptor tyrosine kinases**, *Cell*. 141(7):1117-34.

Llovet JM, Bruix J, (2008). **Molecular targeted therapies in hepatocellular carcinoma**, *Hepatology*. 48(4):1312-27.

Lyman SD, James L, Vanden Bos T, de Vries P, Brasel K, Gliniak B, Hollingsworth LT, Picha KS, McKenna HJ, Splett RR, et al., (1993). **Molecular cloning of a ligand for the flt3/flk-2 tyrosine kinase receptor: a proliferative factor for primitive hematopoietic cells**, *Cell*. 75(6):1157-67.

Lyman SD, James L, Zappone J, Sleath PR, Beckmann MP, Bird T, (1993). **Characterization of the protein encoded by the flt3 (flk2) receptor-like tyrosine kinase gene,** *Oncogene*. 8(4):815-22.

Maroc N, Rottapel R, Rosnet O, Marchetto S, Lavezzi C, Mannoni P, Birnbaum D, Dubreuil P, (1993). **Biochemical characterization and analysis of the transforming potential of the FLT3/FLK2 receptor tyrosine kinase**, *Oncogene*. 8(4):909-18.

Martin GR**,** (1981). **Isolation of a pluripotent cell line from early mouse embryos cultured in medium conditioned by teratocarcinoma stem cells**, *Proc Natl Acad Sci U S A*. 78(12):7634-8.

Matthews W, Jordan CT, Wiegand GW, Pardoll D, Lemischka IR, (1991). **A receptor tyrosine kinase specific to hematopoietic stem and progenitor cell-enriched populations**, *Cell*. 65(7):1143-52.

McCaughan GW, Gorrell MD, Bishop GA, Abbott CA, Shackel NA, McGuinness PH, Levy MT, Sharland AF, Bowen DG, Yu D, Slaitini L, Church WB, Napoli J, (2000). **Molecular pathogenesis of liver disease: an approach to hepatic inflammation, cirrhosis and liver transplant tolerance**, *Immunol Rev*. 174:172-91.

Michalopoulos GK, DeFrances MC, (1997). **Liver regeneration**, *Science*. 276(5309):60-6.

Mishra L, Banker T, Murray J, Byers S, Thenappan A, He AR, Shetty K, Johnson L, Reddy EP, (2009). **Liver stem cells and hepatocellular carcinoma**, *Hepatology*. 49(1):318-29.

Nakao M, Yokota S, Iwai T, Kaneko H, Horiike S, Kashima K, Sonoda Y, Fujimoto T, Misawa S, (1996). **Internal tandem duplication of the flt3 gene found in acute myeloid leukemia,** *Leukemia*. 10(12):1911-8.

Omenetti A, Porrello A, Jung Y, Yang L, Popov Y, Choi SS, Witek RP, Alpini G, Venter J, Vandongen HM, Syn WK, Baroni GS, Benedetti A, Schuppan D, Diehl AM, (2008). **Hedgehog signaling regulates epithelial-mesenchymal transition during biliary fibrosis in rodents and humans**, *J Clin Invest*. 118(10):3331-42.

Organ Procurement and Trasnplantation Network Data, OrganDonor.gov [online], http://organdonor.gov/, (2010).

Park PH, Miller R, Shukla SD, (2003). **Acetylation of histone H3 at lysine 9 by ethanol in rat hepatocytes**, *Biochem Biophys Res Commun*. 306(2):501-4.

Rosnet O, Matteï MG, Marchetto S, Birnbaum D, (1991). **Isolation and chromosomal localization of a novel FMS-like tyrosine kinase gene**, *Genomics*. 9(2):380-5.

Rosnet O, Stephenson D, Mattei MG, Marchetto S, Shibuya M, Chapman VM, Birnbaum D, (1993). **Close physical linkage of the FLT1 and FLT3 genes on chromosome 13 in man and chromosome 5 in mouse,** *Oncogene*. 8(1):173-9.

Rosnet O, Schiff C, Pébusque MJ, Marchetto S, Tonnelle C, Toiron Y, Birg F, Birnbaum D, (1993). **Human FLT3/FLK2 gene: cDNA cloning and expression in hematopoietic cells**, *Blood*. 82(4):1110-9.

Rozen S, Skaletsky HJ, (2000). **Primer3 on the WWW for general users and for biologist programmers ,** *Bioinformatics Methods and Protocols: Methods in Molecular Biology*. 132:365-386

Qin LX, Tang ZY, (2002). **The prognostic significance of clinical and pathological features in hepatocellular carcinoma**, *World J Gastroenterol*. 8(2):193-9.

Salnikov AV, Kusumawidjaja G, Rausch V, Bruns H, Gross W, Khamidjanov A, Ryschich E, Gebhard MM, Moldenhauer G, Büchler MW, Schemmer P, Herr I, (2009). **Cancer stem cell marker expression in hepatocellular carcinoma and liver metastases is not sufficient as single prognostic parameter,** *Cancer Lett*. 275(2):185-93.

Sanz M, Burnett A, Lo-Coco F, Löwenberg B, (2009). **FLT3 inhibition as a targeted therapy for acute myeloid leukemia**, *Curr Opin Oncol*. 21(6):594-600.

Sell S, Leffert HL, (2008). **Liver cancer stem cells,** *J Clin Oncol*. 26(17):2800-5.

Singh A, Settleman J, (2010). **EMT, cancer stem cells and drug resistance: an emerging axis of evil in the war on cancer,** *Oncogene*. Jun 7. [Epub ahead of print]

Si-Tayeb K, Lemaigre FP, Duncan SA, (2010). **Organogenesis and development of the liver,** *Dev Cell*. 18(2):175-89.

Stirewalt DL, Radich JP, (2003). **The role of FLT3 in haematopoietic malignancies,** *Nat Rev Cancer*. 3(9):650-65.

Taub R, (2004). **Liver regeneration: from myth to mechanism,** *Nat Rev Mol Cell Biol*. 5(10):836-47.

Thiede C, Steudel C, Mohr B, Schaich M, Schäkel U, Platzbecker U, Wermke M, Bornhäuser M, Ritter M, Neubauer A, Ehninger G, Illmer T, (2002). **Analysis of FLT3-activating mutations in 979 patients with acute myelogenous leukemia: association with FAB subtypes and identification of subgroups with poor prognosis,** *Blood*. 99(12):4326-35.

Turner AM, Lin NL, Issarachai S, Lyman SD, Broudy VC, (1996). **FLT3 receptor expression on the surface of normal and malignant human hematopoietic cells,** *Blood*. 88(9):3383-90.

Wandzioch E, Kolterud A, Jacobsson M, Friedman SL, Carlsson L**,** (2004). **Lhx2-/- mice develop liver fibrosis**, *Proc Natl Acad Sci U S A*. 101(47):16549-54.

Wu L, Liu YJ, (2007). **Development of dendritic-cell lineages**, *Immunity*. 26(6):741-50.

Villanueva A, Newell P, Chiang DY, Friedman SL, Llovet JM**,** (2007). **Genomics and signaling pathways in hepatocellular carcinoma**, *Semin Liver Dis*. 27(1):55-76.

Yamashita T, Ji J, Budhu A, Forgues M, Yang W, Wang HY, Jia H, Ye Q, Qin LX, Wauthier E, Reid LM, Minato H, Honda M, Kaneko S, Tang ZY, Wang XW, (2009). **EpCAM-positive hepatocellular carcinoma cells are tumor-initiating cells with stem/progenitor cell features**, *Gastroenterology*. 136(3):1012-24.

Yang W, Yan HX, Chen L, Liu Q, He YQ, Yu LX, Zhang SH, Huang DD, Tang L, Kong XN, Chen C, Liu SQ, Wu MC, Wang HY, (2008). **Wnt/beta-catenin**

signaling contributes to activation of normal and tumorigenic liver progenitor cells, *Cancer Res*. 68(11):4287-95.

Yang ZF, Ho DW, Ng MN, Lau CK, Yu WC, Ngai P, Chu PW, Lam CT, Poon RT, Fan ST, (2008). **Significance of CD90+ cancer stem cells in human liver cancer**, *Cancer Cell*. 13(2):153-66.

Yin S, Li J, Hu C, Chen X, Yao M, Yan M, Jiang G, Ge C, Xie H, Wan D, Yang S, Zheng S, Gu J**,** (2007). **CD133 positive hepatocellular carcinoma cells possess high capacity for tumorigenicity**, *Int J Cancer*. 120(7):1444-50.

Zeisberg M, Yang C, Martino M, Duncan MB, Rieder F, Tanjore H, Kalluri R, (2007). **Fibroblasts derive from hepatocytes in liver fibrosis via epithelial to mesenchymal transition,** *J Biol Chem*. 282(32):23337-47.

Zhang W, Yatskievych TA, Cao X, Antin PB, (2002). **Regulation of Hex gene expression by a Smads-dependent signaling pathway,** *J Biol Chem*. 277(47):45435-41.

Zhao R, Duncan SA, (2005). **Embryonic development of the liver**, *Hepatology*. 41(5):956-67.

Zhou B, Shan H, Li D, Jiang ZB, Qian JS, Zhu KS, Huang MS, Meng XC, (2010). **MR tracking of magnetically labeled mesenchymal stem cells in rats with liver fibrosis**, *Magn Reson Imaging*. 28(3):394-9.

7. Appendix

STANDARD SOLUTIONS AND BUFFERS

DEPC-Treated ddH_2O

1ml DEPC

1lt ddH_2O

Stirred in a hood for 1 hour, autoclaved in order to inactivate the DEPC

10x PBS

80 g NaCl

2 g KCl

8,01g $Na_2HPO_4.2H_2O$

2g KH_2PO_4

1 liter ddH_2O pH: 7,2

Working solution (1XPBS) was prepared by diluting 10XPBS by 10 times

50X TAE Buffer

2M Tris Base (242 g)

57,1 ml Glacial Acetic Acid

50mM EDTA

Add to 1 lt by ddH_2O

Working solution (1XTAE) prepared by diluting 50XTAE.

10 X Agarose Gel Loading Dye

0,009g BFB

0,009g XC

2,8mL ddH2O

1,2ml 0,5M EDTA.

Total volume brought to 15ml by adding glycerol, dilute 1:10 in sample prior to loading to electrophoresis gel

10%SDS

100g SDS

1lt ddH_2O

1M Tris

60.55g Tris

300ml ddH2O

21ml 37% HCl

pH adjusted to 8.0 with HCl, total volume brought to 500ml by adding ddH_2O.

0.5M EDTA

93.05g EDTA

300ml ddH2O

pH adjusted to 8.0 with NaOH, total volume brought to 500ml by adding ddH_2O.

30% Acrylamide Mix

145g Acrylamide

5g bis-acrylamide

500ml ddH_2O

Filtered, stored in dark at 4^0C.

SDS-PAGE Running Buffer (5X stock solution)

15g Tris

73,2g Glycine

5g SDS

1lt ddH2O

1X working solution prepared by diluting the 5X SDS-PAGE running buffer 5 times, stored at 4^0C

Bradford Reagent

100 mg Coomassie Brilliant Blue G-250

100 ml 85%phosphoric acid

50 ml 95%EtOH

850 ml ddH_2O

Filtered through Whatman no:1

Lysis Buffer

2M NaCl

1M Tris pH:8.2

0.9% Igepal CA-630 (Sigma, Germany)

10x Protease Inhibitor Cocktail (Roche, Germany)

778.5μl ddH_2O

10X TBS

12.19 g Tris

87,76 g NaCl

pH adjusted to 8, total volume brought to 1lt by adding ddH_2O

1X TBS-T 0.1%

50 ml 10X TBS

450 ml ddH_2O

1ml Tween-20

Total volume brought to 500ml by adding ddH_2O

Blocking Solution for Western Blot (5%)

2,5 g milk powder

50mL 1X TBS-T(0.1%)

5% BSA Blobking Solution

0.5g BSA

10mL 1X TBS-T(0.1%)

Blocking Solution for Immunohistochemistry and Immunoflourescence Staining

4 μl 2% BSA

4 μl 1X PBS

20 μl Tween-20

1XPBS-T (0.1%)

500ml 1XPBS

0.5ml Tween-20

Cracking Buffer (2X Protein Loading Buffer)

50mM Tris HCl pH: 6,8

2mM EDTA pH: 6,8

1% SDS

20% Glycerol

0,02% BFB

Add 1% ß-mercaptoethanol prior to use

Coomassie Blue Staining Solution:

0,25 g coomassie brilliant blue

45 ml Methanol

45 ml ddH_2O

10 ml glacial acetic acid

5X Running Buffer

15 g Tris base

72 g Glycine

5 g SDS

1 liter ddH_2O

Diluted to 1X prior to use

Semi-dry Transfer Buffer

2,5 g glycine

5,8 g Tris base

0,37 g SDS

200 ml methanol

800 ml ddH_2O

Wet Transfer Buffer

9g Tris Base

43.2g Glycine

300mL Methanol

1.5mL 10%SDS

Complete volume to 1.5L.

Destaining Solution

100 ml methanol

35 ml acetic acid

365 ml ddH_2O

Sodium Citrate Buffer

10mM Sodium Citrate, 0.05% Tween-20

Adjust pH to 6.0